

CFD ANALYSIS OF AIRFLOW FOR CAPTURE EFFICIENCY OF RESIDENTIAL  
RANGE-HOODS

A Thesis

by

SAM CUU NGUYEN

Submitted to the Graduate and Professional School of  
Texas A&M University  
in partial fulfillment of the requirements for the degree of  
MASTER OF SCIENCE

Chair of Committee,	Michael B. Pate
Committee Members,	Astrid Layton
	Maria D. King
Head of Department,	Guillermo Aguilar

August 2021

Major Subject: Mechanical Engineering

Copyright 2021 Sam Cuu Nguyen

## **ABSTRACT**

HVAC ventilation systems play an important role in maintaining healthy indoor air quality levels by removing air pollutants to the outdoors. In order to evaluate the ability of domestic range-hoods to remove contaminated air from kitchen environments, the American Society for Testing and Materials (ASTM) developed the ASTM-E3087 standard (Standard Test Method for Measuring Capture Efficiency of Domestic Range-Hoods). This standard was used to build and develop a well-instrumented test chamber at the RELIS Energy Efficiency Laboratory (REEL) for the purpose of measuring and evaluating the capture efficiency (CE) of different range-hoods following procedures that comply with the standard. A shortcoming of evaluating range-hood capture efficiency by using the test facility is that the experiments are time consuming. In addition, parts of the test facility and the ASTM standard procedures, may in fact need further evaluations for improvements. Therefore, this study focused on designing and developing a computational fluid dynamics (CFD) model based on the CE test procedures specified in ASTM-E3087, with the goal of simulating the space environment and the boundary conditions of the actual test chamber located at REEL.

An important step before the CFD model can be applied is validating it, which means showing that there is good agreement between the simulation model output and experimental measurements of CE. In support of this study and the above CFD model validation, multiple CE experiments were conducted on a typical residential kitchen range-hood. For this purpose, a Venmar under-cabinet range-hood, Inspira IU600ES30BL, was selected for testing and modeling. These tests and simulations were performed at three different experimental test conditions, representing three fan operating speeds and thus

different air flowrates (in CFM, cubic-feet-per-minute) and CO<sub>2</sub> gas injection rates (in standard l/m, liters-per-minute). During each experimental test, CO<sub>2</sub> concentrations were measured using three sensors placed at three different locations according to the ASTM E3087-18 standard. These measured CO<sub>2</sub> concentrations were in turn used to calculate the capture efficiencies at the special test conditions. Next, the CFD simulation model was used to predict values of CO<sub>2</sub> concentrations at the same three test conditions, followed by calculations of CE values. Of special importance are the CE differences between the results of the CFD simulations and the experiments for the three cases, which were found to be 0.01%, 2.73%, and 0.14%. Based on the closeness of these results, the CFD model was considered validated, so that it could in fact be used as a tool for analyzing and evaluating CE methodologies and test facilities.

Once the CFD model was validated, it was then used to analyze the distribution of CO<sub>2</sub> concentration inside the chamber for the purpose of evaluating the optimum chamber location for CO<sub>2</sub> trace gas sampling, based on a location where the sample value is representative of the chamber as a whole. The results of this evaluation showed that the sampling location that is specified in the ASTM-E3087 standard is in fact in a region of uniform CO<sub>2</sub> distributions, meaning the standard location is representative of the chamber as a whole. Quantitatively, the capture efficiency at the standard-specified location is about 3% to 5% higher than those CE values based on sampling locations near the walls and door of the chamber.

A second study that made use of the validated CFD simulation model was to investigate the effect that the volume of the test chamber has on CE testing and measurements. This investigation was extremely important because the ASTM-E3087

standard does not specify exact chamber dimensions or volumes, and tests performed on the same range-hood at the same test conditions in two different facilities of different volumes produced significantly different CE values, which was a surprising outcome. Using the CFD simulation model, CE values were determined for several chambers with different volumes, and the results showed that measured capture efficiency decreases as the volume of the chamber increases. In one example, as the volume was decreased by 65%, the capture efficiency went up by as much as 27 %. This particular example of a volume decrease was a comparison of the actual REEL test chamber and the smaller standard minimum-dimensions chamber specified in ASTM-E3087, which is a volume lower limit. Based on this important result, it is highly recommended that the standard specifies an exact chamber size for CE tests rather than specifying a minimum-size chamber.

## **DEDICATION**

I would like to dedicate this thesis to my loving parents who have sacrificed their priorities and always wanted to provide me with the best opportunities to become who I am today, and who unconditionally loved, supported, and believed in me throughout my life and academic years; to my brother, Jason, for being a great mentor and mental support in my life; to my grandparents and the whole family for their love and support throughout my life.

To my girlfriend Danielle who has always constantly support and encouraged me which helps me overcome the challenges throughout my academic years.

To all my friends for being such a great part of my journey and for always believing in me throughout my graduate studies. Thank you.

## **ACKNOWLEDGEMENTS**

I would like to thank Dr. Pate, my committee chair, for his constant support and guidance through my master's degree and this thesis project, and for giving me the opportunity to be a part of REEL and to pursue the master's degree.

To Dr. Layton and Dr. King for willing accepting to be a part of my graduate committee; and for the support through my graduate studies.

Finally, I would like to thank my friends and coworkers Edgar, Mario, Tristan, and Troy for their support through this research.

## **CONTRIBUTORS AND FUNDING SOURCES**

### **Contributors**

This thesis work was supervised by a graduate committee comprised of Professor PATE (advisor) and Professor LAYTON of the Department of Mechanical Engineering and Professor KING of the Department of Biological and Agricultural Engineering.

### **Funding Sources**

This graduate study was supported by an assistantship from Dr. PATE and the Energy System Laboratory.

## NOMENCLATURE

ASTM	American Society for Testing and Materials
$C_{ambient}$	CO <sub>2</sub> Concentration in the Ambient Air Inlet (ppm)
$C_{chamber}$	CO <sub>2</sub> Concentration inside Chamber (ppm)
$C_{exhaust}$	CO <sub>2</sub> Concentration in Chamber Exhaust (ppm)
CE	Capture Efficiency (%)
$CE_{CFD}$	CFD Simulation CE value (%)
$CE_{Experimental}$	Experimental CE Value (%)
CFM	Cubic Feet per Minute – Measure of Volumetric Flow Rate
CO <sub>2</sub>	Carbon Dioxide
DIF	Percentage Difference (%)
HS	High Fan Speed Setting (CFM)
HVI	The Home Ventilating Institute
IR	Injection Rate (l/m)
LBNL	Lawrence Berkeley National Lab
LS	Low Fan Speed Setting (CFM)
MS	Medium Fan Speed Setting (CFM)
$\dot{m}$	Mass Flow Rate (kg/s)
$\rho$	Density (kg/m <sup>3</sup> )
$Q_{hood}$	Operating Speed of the Range-hood (CFM)
REEL	RELLIS Energy Efficiency Laboratory
RHCE	Range Hood Capture Efficiency (%)



$T_{ss}$	Estimated Time Required to Achieve Steady-state (min)
$V$	Volume of Test Chamber ( $ft^3$ )
$\dot{V}$	Volumetric Flow Rate ( $m^3/s$ )

# TABLE OF CONTENTS

	Page
ABSTRACT -----	ii
DEDICATION-----	v
ACKNOWLEDGEMENTS -----	vi
CONTRIBUTORS AND FUNDING SOURCES -----	vii
NOMENCLATURE -----	viii
TABLE OF CONTENTS -----	x
LIST OF FIGURES -----	xii
LIST OF TABLES -----	xiv
CHAPTER 1. INTRODUCTION -----	1
CHAPTER 2. DESCRIPTION OF CAPTURE EFFICIENCY TEST FACILITY AND METHODOLOGY -----	5
2.1 Experimental Measurement Facility and Procedures -----	5
2.2 Calculation Procedures for Capture Efficiency (CE) -----	7
2.3 Test Conditions -----	8
2.4 Burner Assembly and CO2 Injection-----	9
2.5 Range-hood Fan Unit -----	11
CHAPTER 3. DEVELOPMENT OF THE CFD SIMULATION MODEL -----	13
3.1 Three-Dimensional Model of the REEL CE Test Chamber -----	13
3.2 Overview of Computational Processes:-----	15
3.3 Computational Mesh-----	16
3.4 Computational Equations -----	17
3.5 Boundary Conditions -----	18
CHAPTER 4. VALIDATION OF CFD MODEL USING EXPERIMENTAL CE VALUES -----	21

4.1	Experimental Results Summary-----	21
4.2	CFD Numerical Results Summary -----	23
4.3	Validation of The CFD Simulation Model Using Experimental Data-----	23
CHAPTER 5. CFM MODEL ANALYSIS OF CO <sub>2</sub> CONCENTRATION DISTRIBUTIONS AND SAMPLING LOCATIONS -----		28
5.1	Overview -----	28
5.2	Methodology -----	29
5.3	Summary of Results and Discussion -----	30
CHAPTER 6. IMPACT OF CHAMBER VOLUME ON CAPTURE EFFICIENCY MEASUREMENTS -----		41
6.1	Background and Methodology -----	41
6.2	Summary of Results and Discussion -----	45
CHAPTER 7. CONCLUSIONS -----		51
REFERENCES -----		54

## LIST OF FIGURES

	Page
FIGURE 1: A FRONT SCHEMATIC FOR THE TESTING CHAMBER AT REEL SHOWING THE THREE CO <sub>2</sub> SAMPLING SENSOR LOCATIONS (MODIFIED FROM ASTM E3087-18) [1] .....	6
FIGURE 2: A SIDE SCHEMATIC FOR THE TESTING CHAMBER AT REEL SHOWING THE THREE CO <sub>2</sub> SAMPLING SENSOR LOCATIONS (MODIFIED FROM ASTM E3087-18) [1] .....	7
FIGURE 3: EXPERIMENTAL ARRANGEMENT OF THE ACTUAL CE TEST CHAMBER AT REEL 10	
FIGURE 4: PLUME DIFFUSION TRACER GAS EMITTER ASSEMBLY (ADAPTED FROM ASTM E3078) [1] .....	11
FIGURE 5: VENMAR INSPIRA IU600ES30BL UNDER-CABINET RANGE-HOOD (REPRINTED FROM VENMAR) [10].....	12
FIGURE 6: SIMPLIFIED 3D MODEL OF THE CE TEST CHAMBER WITH COMPONENTS .....	15
FIGURE 7: THREE MAJOR STEPS IN A CFD SIMULATION .....	16
FIGURE 8: MESH OF THE TEST CHAMBER USED IN THE COMPUTATIONAL ANALYSIS .....	17
FIGURE 9: CFD SIMULATIOPN AND EXPERIMENTALLY MEASURED CAPTURE EFFICIENCY COMPARISON .....	25
FIGURE 10: A SCHEMATIC OF THE VOLUME VONTROL OF THE CFD MODEL SHOWING THE THREE ADDITIONAL CO <sub>2</sub> CONCENTRATION MEASUREMENT LOCATIONS ALONG WITH THE ORIGINAL CHAMBER LOCATION .....	29
FIGURE 11: COMPARISON OF CALCULATED CE RESULTS AT THE FOUR DIFFERENT SAMPLING LOCATIONS .....	31
FIGURE 12: DISTRIBUTIONS OF STEADY-STATE CO <sub>2</sub> CONCENTRATION ON THE VERTICAL CROSS-SECTIONAL PLANES (TOP SIDE PLOT) AND THE HORIZONTAL CROSS-SECTIONAL PLANES (BOTTOM SIDE PLOT) FOR THREE SIMULATIONS.....	36
FIGURE 13: DISTRIBUTIONS OF STEADY-STATE CO <sub>2</sub> CONCENTRATIONS ON HORIZONTAL CROSS-SECTIONAL PLANES AT FOUR DIFFERENT HEIGHTS.....	39
FIGURE 14: BAR-CHART COMPARISON OF THE TOTAL VOLUME OF THE FOUR CHAMBERS	44

FIGURE 15: COMPARISON OF CO<sub>2</sub> CONCENTRATIONS AT THREE STANDARD SPECIFIED SAMPLING LOCATIONS FOR THE FOUR CHAMBERS VOLUMES..... 47

FIGURE 16: COMPARISON OF CALCULATED RANGE-HOOD CE VALUES FOR THE FOUR CHAMBER VOLUMES..... 47

FIGURE 17: CALCULATED RANGE-HOOD CE VALUES VARYING WITH VOLUME CHANGES ASSOCIATED WITH THE FOUR SIMULATIONS ..... 49

## LIST OF TABLES

	Page
TABLE 1: TESTING COMBINATIONS FOR RANGE-HOOD SPEED SETTINGS AND CO <sub>2</sub> INJECTION RATES .....	9
TABLE 2: SUMMARY OF THE MAJOR COMPONENTS MODELED IN THE CFD SIMULATION ..	14
TABLE 3: CO <sub>2</sub> MASS FLOW RATE TEST CONDITIONS.....	19
TABLE 4: BOUNDARY CONDITIONS FOR THE CFD SIMULATIONS.....	20
TABLE 5: EXPERIMENTAL TEST RESULTS CONSISTING OF CO <sub>2</sub> CONCENTRATIONS AND CE VALUES .....	22
TABLE 6: CFD PREDICTED VALUES OF CO <sub>2</sub> CONCENTRATIONS AND CE VALUES.....	23
TABLE 7: PERCENTAGE DIFFERENCE BETWEEN CFD PREDICTED VALUES AND EXPERIMENTAL DATA.....	24
TABLE 8: PERCENTAGE DIFFERENCE BETWEEN CFD PREDICTED VALUES AND EXPERIMENTAL DATA.....	26
TABLE 9: COMPARISON SUMMARY OF CO <sub>2</sub> CONCENTRATIONS AND CE AT FOUR LOCATION BASED ON CFD SIMULATIONS .....	30
TABLE 10: COMPARISON OF CALCULATED CAPTURE EFFICIENCY (CE) AT SAMPLING LOCATIONS BY USING THE CHAMBER LOCATION CE AS SPECIFIED IN ASTM-E3087 AS A REFERENCE.....	32
TABLE 11: COMPARISON OF DIMENSIONS AND VOLUMES FOR FOUR CHAMBERS .....	43
TABLE 12: SUMMARY OF CO <sub>2</sub> CONCENTRATIONS AND CALCULATED CE VALUES FOR FOUR DIFFERENT CHAMBER SIZES USING THE CFD SIMULATION MODEL .....	46

## CHAPTER 1. INTRODUCTION

The purpose of local ventilation systems, such as kitchen range-hood fans, are to maintain healthy indoor environments by rejecting stale or contaminated air to the outdoors before it is inhaled or mixed with air in other parts of the indoor space.

Air pollutants from cooking activities and building material outgassing can be unhealthy to breathe when poor ventilation exists. With regards to cooking activities, air pollutants emitted include carbon monoxide, carbon dioxide, formaldehyde, and other harmful pollutants from either high temperature heating of different food ingredients or from using combustion heat sources such as gas, oil, or wood. In order to mitigate this issue, building requirements exist to ensure that efficient range-hood and fan units are installed in kitchens. Furthermore, ASTM-E3078 was developed by ASTM for the purpose of testing and evaluating the ability of domestic range-hoods to remove contaminants that are released in the kitchen environments by using a measurable parameter called capture efficiency (CE). The ASTM-E3087 standard defines the CE of a range-hood as the percentage of the total pollutants emitted that are captured and/or removed by the kitchen range-hood fan.

An integral part of the study reported herein is the use of an experimental range-hood test chamber located at the RELIS Energy Efficiency Laboratory (REEL). This facility was designed and built for measuring and analyzing range-hood capture efficiencies following the standardized procedures specified in ASTM 3087-18. In this CE chamber, the mixing air is removed by the range-hood fan and the indoor air is supplied through an open vent on the chamber ceiling, while CO<sub>2</sub> is injected as a tracer gas to

simulate pollutants released during cooking. Sensors for measuring CO<sub>2</sub> concentrations are placed in the chamber space and at the inlet/exit and then using equations from the standard, a CE value is calculated for any set of test conditions.

A shortcoming of experimental CE testing in accordance with the standard is that the experiments are time consuming, and building a test chamber with components and instruments is costly. For example, it can take as long as 4 to 5 hours to complete a CE test for any single specified condition, depending on range-hood fan operating speeds and injection rates of the CO<sub>2</sub> tracer gas. Specifically, time is required to allow the chamber air to reach steady state as well as for the top surfaces of the hot emitter plates to reach the desired temperature as specified in ASTM-E3087. The above effort is for only one test point, and to evaluate any given range-hood unit, multiple test conditions are necessary. To complement the above experimental effort, a computational fluid dynamics (CFD) simulation model was developed to predict CO<sub>2</sub> distributions and CE values for the aforementioned ventilation system following procedures that comply with the ASTM-E3087 standard. A comparison of the experimental data and the CFD results validated the ability of the simulation model to accurately predict CO<sub>2</sub> distributions and CE values when proper conditions and assumptions are applied.

There are several advantages to using the CFD model to simulate CE testing, with one major benefit being that it reduces the time of performing CE tests, which as noted before can be extensive for experiments. Furthermore, the CFD simulations can be used to evaluate changes to a theoretical test chamber by simulating the physical conditions,



such as chamber sizes, as if it were an actual chamber and then evaluating the effect of a new chamber on measured CE values.

The above CFD simulation model, which is a major part of this study along with using it for design and analysis, was developed by using Fluent software with turbulence mixing, along with the fluid flow being air and a CO<sub>2</sub> tracer gas. Imposed on the CFD model so as to specifically comply with ASTM-E3087 are chamber components, heat sources at special temperatures, simulation boundaries, and depressurization of the air inlet. In addition, multiple models used dimensions of both actual experimental test chambers and fictitious chambers. As a final note, the predicted CE results using the CFD simulations were compared with the experimental measurements for validation.

Other than the REEL test facility reported and used herein, there has been only one other CE test facility, that has been constructed to perform CE experiments by using test procedures specified in ASTM-E3087. This facility was built and operated by Lawrence Berkeley National Lab (LBNL). Of special importance for the study reported herein, CE test results reported by LBNL were shown to be higher than those CE values measured by REEL, even though each facility utilized the same test conditions and the same range-hood unit. This disagreement was quite surprising considering that both facilities were built and operated by following the same ASTM-E3087 standard and, as mentioned, the same range-hood fan unit was tested. It was hypothesized that the reason for this difference in measured CE values is that the standard does not require a specific chamber volume, but rather only puts a limit on the minimum size. As a result, even though the two chambers satisfy the standard, they were built with different volumes, which in fact

resulted in different CE values being measured. Because it is not easy to vary the actual chamber volume, the purpose of this study is to use a validated CFD simulation model to identify chamber volume as a possible influence on range-hood CE results. Furthermore, this study could lead to recommendations for improvements in the ASTM-E30787 standard.

## **CHAPTER 2. DESCRIPTION OF CAPTURE EFFICIENCY TEST FACILITY AND METHODOLOGY**

The experimental test facility for measuring CE values that presently exists at REEL is an important part of the study reported herein. Firstly, the facility was used to experimentally test and measure the CE performance of the range-hood fan unit that was first tested at LBNL, which allows for a comparison of CE measurements from two different test facilities. Secondly, this test facility was modeled in the CFD simulation, with the experimental test results for CE then being used to validate this CFD model.

### **2.1 Experimental Measurement Facility and Procedures**

The test facility at REEL was designed and built following guidance in ASTM-E3087, Standard Test Method for Measuring Capture Efficiency of Domestic Range-hoods. This standard was developed for the purpose of providing a uniform methodology for testing and evaluating the capture efficiency (CE) performance of kitchen range-hoods. With regards to the physical layout of this facility, there are two focus areas. The first focus area is the test chamber and its many components, which simulates a real-world kitchen. As shown in Figure 1 (from a front perspective) and 2 (from a side perspective), it consists of an air-tight chamber constructed with countertops, cabinets, and simulated burner assemblies along with a range-hood fan unit and exhaust ducting. The second focus area is sensors, a CO<sub>2</sub> delivery system, and data acquisition. Specifically, CO<sub>2</sub> sensors were installed at three different locations, namely the ambient air inlet, the test chamber, and the exhaust ducting of the chamber. The CO<sub>2</sub> sampling locations specified in ASTM-E3087 are shown in Figure 1 and 2. The signal and data were recorded using the different

CO<sub>2</sub> sensors and thermocouples through a National Instruments Data Acquisition system (DAQ). This data was then manually taken by the technician and inputted into LabVIEW software. The CO<sub>2</sub> tracer gas, which represents contaminants, is delivered to the test chamber via tubing, emitter plates, control valves, a flow measuring device and storage tanks.

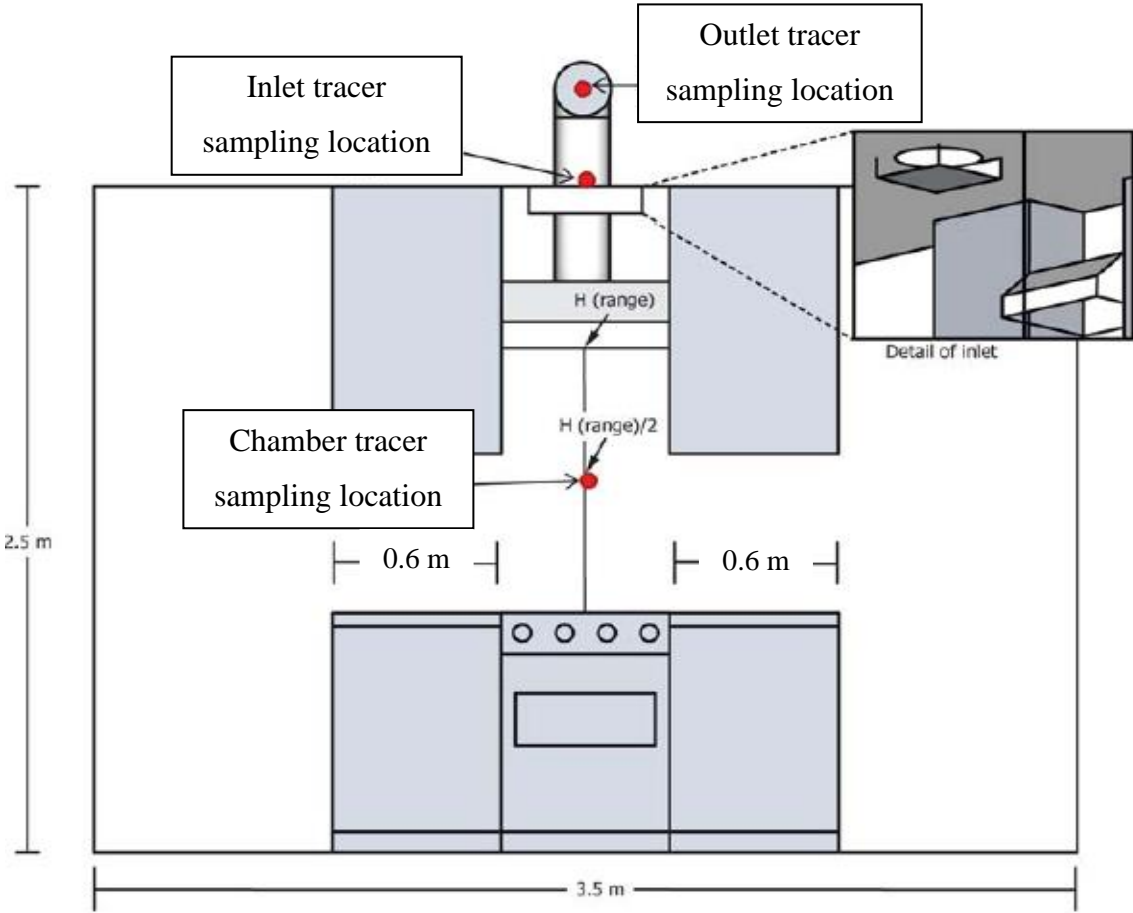


Figure 1: A front schematic for the testing chamber at REEL showing the three CO<sub>2</sub> sampling sensor locations (Modified from ASTM E3087-18) [1]

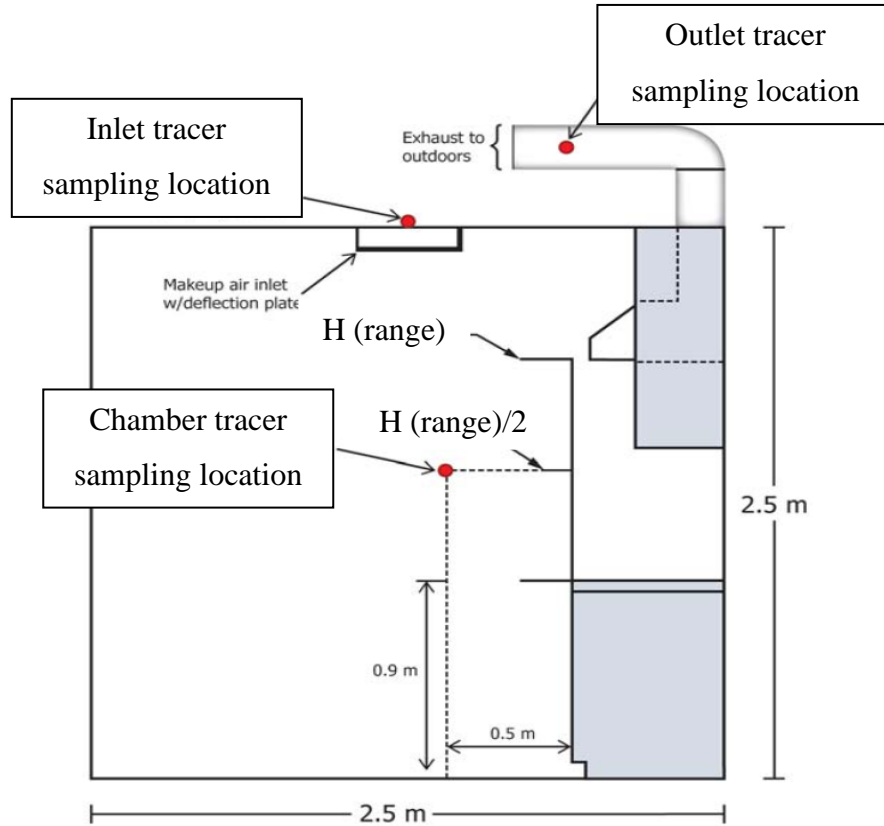


Figure 2: A side schematic for the testing chamber at REEL showing the three CO<sub>2</sub> sampling sensor locations (Modified from ASTM E3087-18) [1]

## 2.2 Calculation Procedures for Capture Efficiency (CE)

According to the ASTM standard, the range-hood capture efficiency (CE) is determined by injecting a known volumetric flowrate of tracer-gas (CO<sub>2</sub>) into the simulated kitchen chamber and then measuring the concentrations of the CO<sub>2</sub> tracer gas at three locations, namely the test chamber, the ambient air inlet, and the exhaust ducting. Next, the CO<sub>2</sub> concentration measurement values at the three locations are plugged into Equation 1 as follows.

$$CE = \frac{C_{exhaust} - C_{chamber}}{C_{exhaust} - C_{ambient}} \quad [1]$$

The terminology used in Equation 1 above, consist of  $C_{ambient}$ ,  $C_{chamber}$ , and  $C_{exhaust}$ , which represent measured concentrations of CO<sub>2</sub> in the ambient air inlet of the test chamber, in the test chamber, and in the exhaust ducting, respectively. As noted previously, the capture efficiency or CE is defined as the ratio of the contaminations that are captured or exhausted to the total contaminants emitted from the stovetop.

The ASTM standard also specifies that steady-state conditions must be reached by having four complete room air changes before taking CO<sub>2</sub> concentration measurements. The steady-state time can be calculated by using Equation 2 as follows.

$$T_{SS} = 4 \times \frac{V_{chamber}}{Q_{hood}} \quad [2]$$

where,  $T_{SS}$  is the steady-state time (min.),  $V_{chamber}$  is the total volume of the chamber ( $ft^3$ ),  $Q_{hood}$  is the operating speed of the range hood (CFM), and (4) is the constant representing four full air changes.

### **2.3 Test Conditions**

As a major part of the study reported herein, the capture efficiency for a selected sample range-hood was measured at three different operating speeds and three different tracer-gas injection rates. The three different speed settings are 160 CFM (low speed), 250 CFM (medium speed), and 300 CFM (high speed); and the three injection rates, which are each associated with a fan speed, are 20 l/m, 30 l/m, and 40 l/m, respectively. Table 1 summarizes the operating speeds and the injection rates used for testing the sample unit. It should be noted that the fan unit and test conditions were selected so that the resulting

data could be compared to the previously mentioned CE data from LBNL. In addition, this broad data set will allow for a thorough validation of the CFD model simulation.

Table 1: Testing Combinations for Range-hood Speed Settings and CO<sub>2</sub> Injection Rates

<b>Test Combination</b>	<b>Speed Setting</b>	<b>Tested Injection Rate</b>
<b>1</b>	160 CFM (LS)	20 l/m
<b>2</b>	250 CFM (MS)	30 l/m
<b>3</b>	300 CFM (HS)	40 l/m

#### **2.4 Burner Assembly and CO<sub>2</sub> Injection**

As noted previously, the CE test chamber used for measuring capture efficiency was designed and constructed at the RELIS Energy Efficiency Laboratory (REEL) by following guidelines presented in ASTM 3087-18 standard. Because of the importance of the simulated burners and CO<sub>2</sub> injection assembly, additional descriptions and understanding are appropriate. The actual experimental arrangement can be seen in Figure 3.



Figure 3: Experimental Arrangement of the actual CE test chamber at REEL

As noted previously, inside the chamber is a simulated cook-stove countertop, and it has two heating elements and two custom built plume-diffusion emitter plates on its top surface. These two emitter plates were specially designed following the ASTM E3087-18 standard to simulate the flow of pollutants ( $\text{CO}_2$  in this case) generated during cooking activities due to the convective flow phenomena. The temperature of the surfaces of two plates were set to  $160^\circ\text{C} \pm 10^\circ\text{C}$  and remained constant during the experiment by using and controlling two voltage variac transformers. Figure 4 is a schematic drawing of the emitter plates as reprinted from ASTM E3080-18.



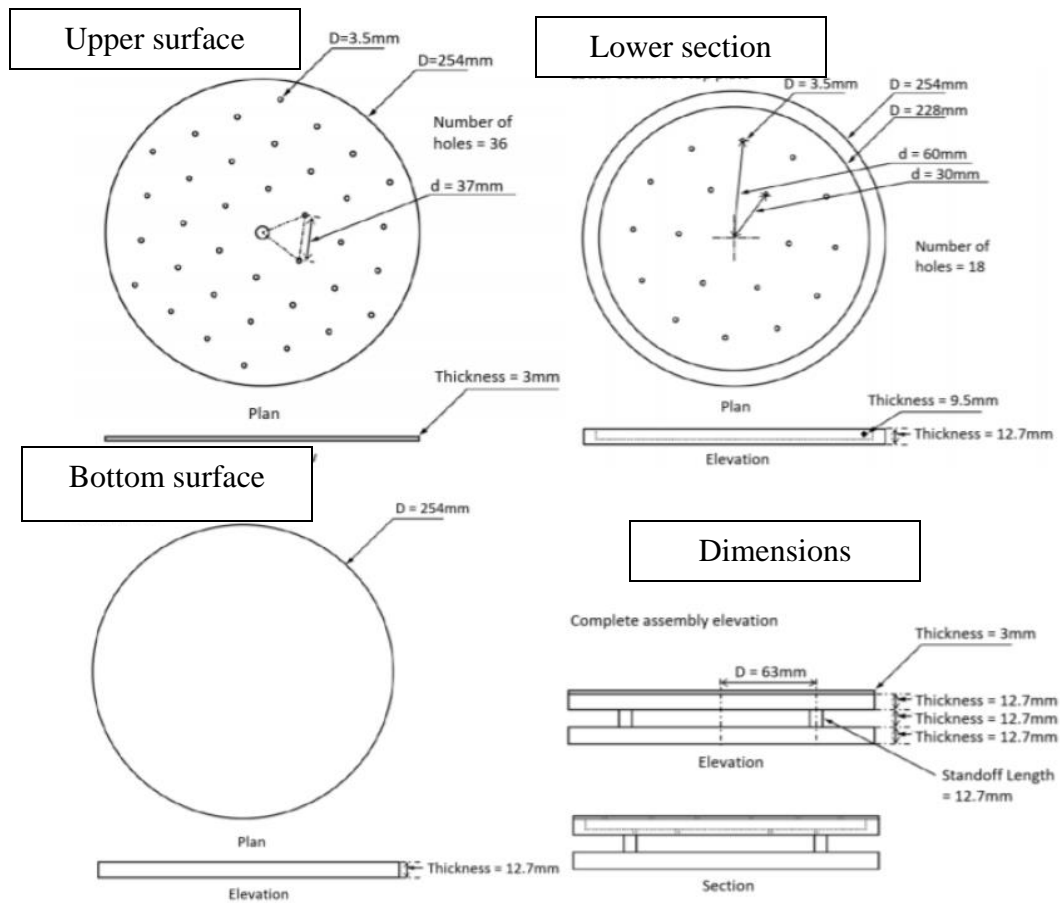


Figure 4: Plume Diffusion Tracer Gas Emitter Assembly (Adapted from ASTM E3078) [1]

Connected to the above emitter plates is a CO<sub>2</sub> injection system consisting of lines, a flow control valve, a flow meter, and a CO<sub>2</sub> storage tank. This system was designed for precision CO<sub>2</sub> injection during any CE test.

## 2.5 Range-hood Fan Unit

A commercially available range-hood was selected for analysis of range-hood CE following the standardized procedures specified in the ASTM. This unit was selected because it is typical of those found in residential homes, plus it is the same type tested for

CE by LBNL. Specifically, it is the Venmar Inspira IU600ES30BL under-cabinet range-hood shown in Figure 5. The range-hood fan was tested for those test combinations listed in Table 1 by using a vertical configuration with a rectangular discharge of 3¼” x 10”. Note that this fan and its test conditions were used in the CFD simulation model that produced CO<sub>2</sub> concentrations at the three locations and hence a simulated CE value.



Figure 5: Venmar Inspira IU600ES30BL Under-cabinet Range-hood (Reprinted from Venmar) [10]

## **CHAPTER 3. DEVELOPMENT OF THE CFD SIMULATION MODEL**

This chapter describes the development of the CFD simulation model of the actual capture efficiency (CE) test facility located and operated at REEL, with the model goal being to predict CE results consistent with those measured using this facility. First, the three-dimensional model of the test chamber and its major components used in the simulation are described. Then, the computational analysis as validated in this study will be detailed and explained.

### **3.1 Three-Dimensional Model of the REEL CE Test Chamber**

Much of the actual test facility was modeled as part of the CFD analysis, however, other components were not considered in the CFD model as they do not affect the CE results or the CO<sub>2</sub> distribution in the chamber that is used to measure the CE. Examples of these excluded components are the data acquisition system, the CO<sub>2</sub> analyzer, CO<sub>2</sub> mass controller, and other minor components installed following ASTM-E3087. The major components that were modeled in the CFD analysis, and thus considered for simulations, are listed in Table 2, with the common theme being that each component can affect the value of the CE.

Table 2: Summary of the Major Components Modeled in the CFD Simulation

<b>Identifier Numbers</b>	<b>Main Components</b>	<b>Quantity</b>
<b>1</b>	Countertop	1
<b>2</b>	Burner (heater plate)	2
<b>3</b>	Emitter plate	2
<b>4</b>	Exhaust system (Range hood and duct)	1
<b>5</b>	Side cabinet	2
<b>6</b>	Inlet box cover	1
<b>7</b>	CO <sub>2</sub> tube line	2

In this CFD analysis, a 3D model of the test chamber and the Table 2 components were duplicated by using SolidWorks software, while ensuring that the dimensions of the actual test chamber as built and installed at REEL were included, following the ASTM-E3087 procedures. The 3D model was simplified by removing the curvature of the range hood/exhaust ducts and the filters on the range-hood and at the chamber inlet. As a result, it was possible to reduce the number of mesh elements and nodes, as well as shortening the time to reach a convergence state, which in turn reduces errors output by the software. For the next step in the CFD simulation, the total air volume of the 3D model was extracted and then imported into Fluent software. The simplified 3D model of the CE test chamber with major components, as identified in Table 2, are showcased in the following Figure 6.

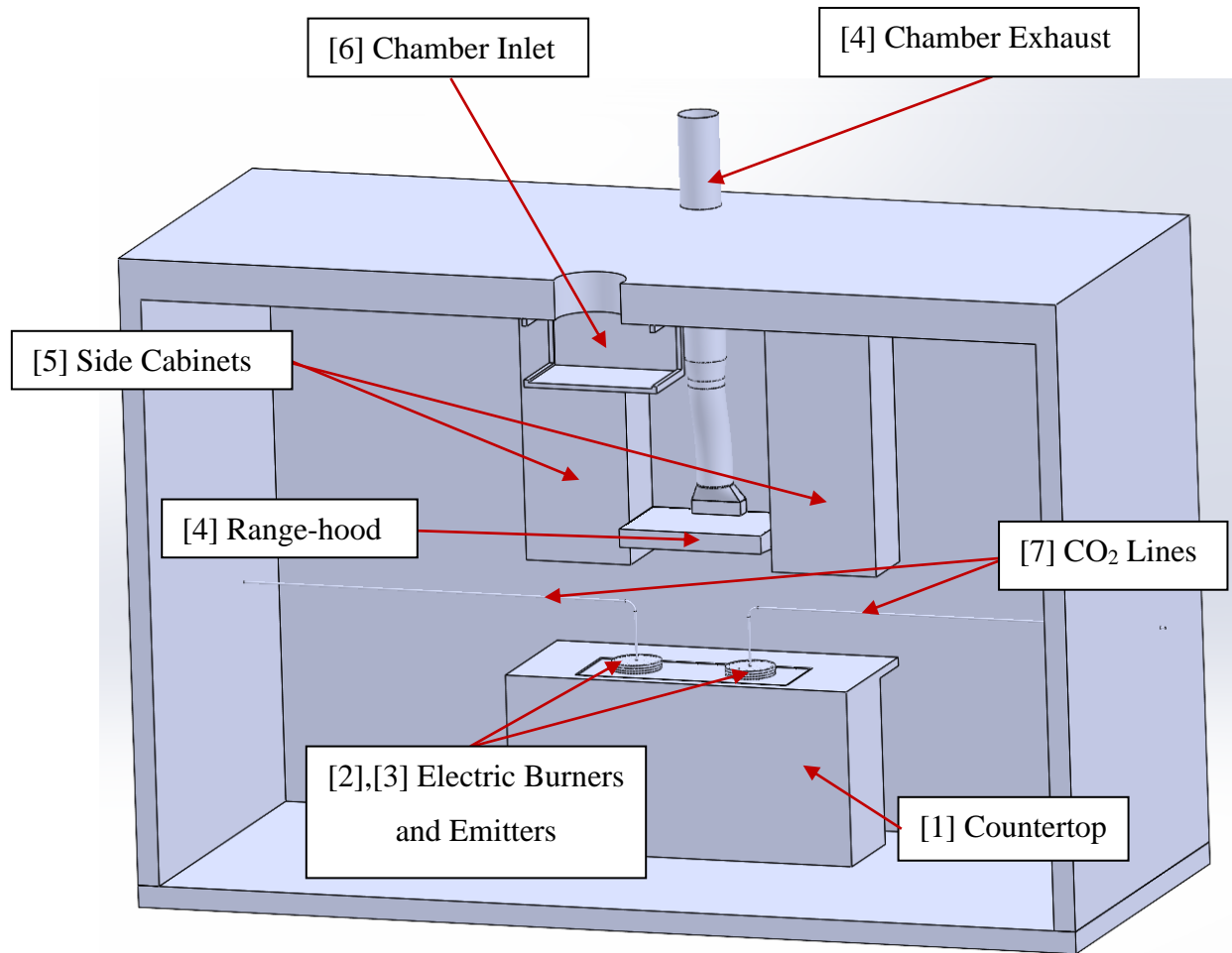


Figure 6: Simplified 3D Model of the CE Test Chamber with Components

### 3.2 Overview of Computational Processes:

Three major steps were performed to complete the CFD simulation of the capture efficiency testing facility, namely pre-processing, simulation solving, and post-processing. The first step, namely the pre-processing, includes defining the major problem and preparing for the simulation. After importing the aforementioned 3D model and generating the meshing model, the second step is solving the simulation by setting up the equations, fluid properties and the boundary conditions. Next, the program solves the equations for the computational model by using the iterative procedure. It is important to

note that the model must be designed so as to simulate the actual environment and conditions of the test chamber in order to produce accurate and consistent results. Finally, the last step, namely the post-processing, includes analyzing the data and results and visually observing the plots to define the CO<sub>2</sub> concentration distributions. A block diagram that summarizes these three major steps is presented in Figure 7.

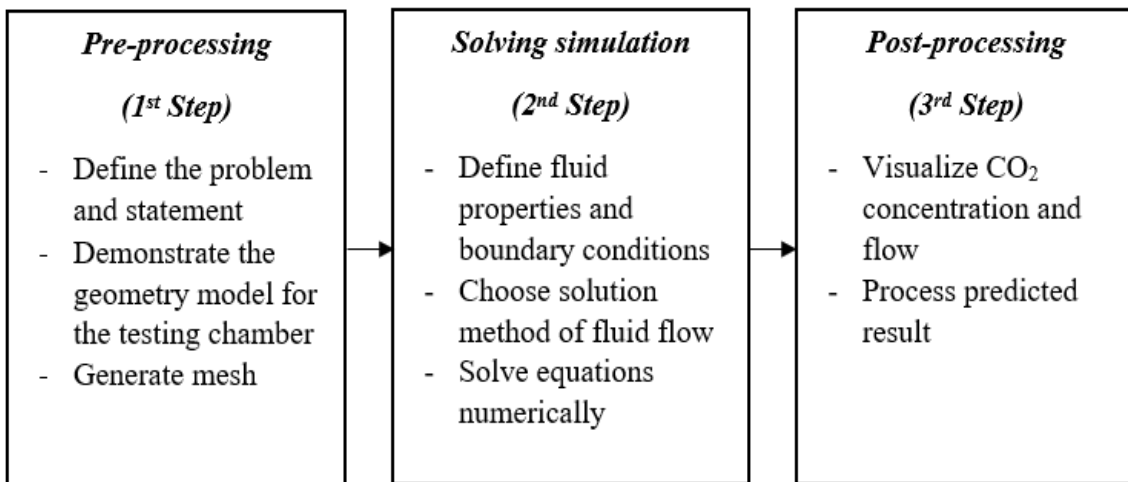


Figure 7: Three Major Steps in a CFD Simulation

### 3.3 Computational Mesh

After importing the 3D model, the next step of the computational analysis is to define a mesh for the model control volume. The mesh for the 3D model of the aforementioned actual CE test facility was prepared by using the Ansys Meshing tool. The mesh consisted of numerous tetrahedral cells, due to the complex shape of the range hood and emitter plates. The element order was set to linear, and the element size was set to 7.5 inches with a smooth transition setting to ensure high quality for the mesh and accurate simulation results. Applying these settings to the control volume of the CFD model

resulted in a total of 2.7 million nodes and 9.5 million elements for computational cells. The mesh developed for use herein is shown in Figure 8.

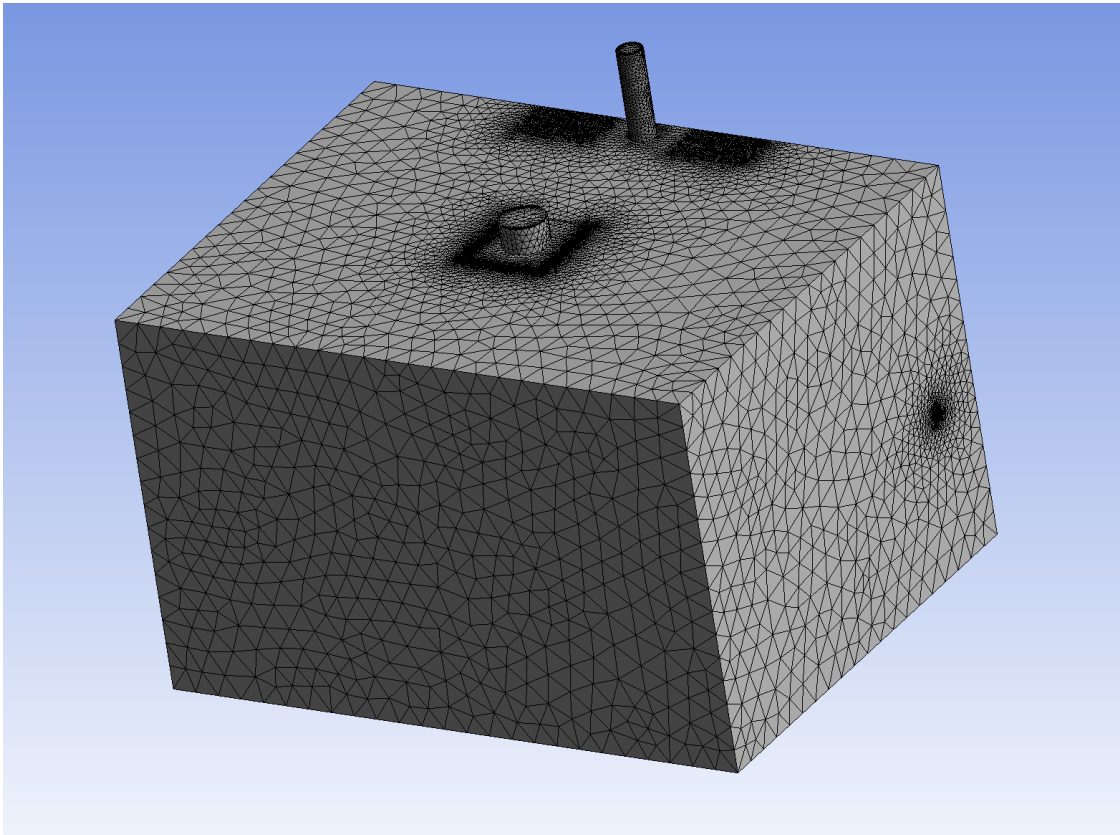


Figure 8: Mesh of the Test Chamber used in the Computational Analysis

### **3.4 Computational Equations**

For this computational analysis, the CFD model is comprised of a 3D model with the Navier-Stokes equation representing the turbulent flow inside of the domain chamber. Of special importance, the results of the simulations must define the CO<sub>2</sub> concentration distributions inside of the chamber; hence, species transport equations are also considered in order to complete the simulation. There are several turbulence models available, with the  $k - \epsilon$  model and  $k - \omega$  models being the most common and accurate for ventilation

system simulations. In this study, the chosen computational model was the realizable  $k - \varepsilon$  model that contains an alternative formulation for the turbulent viscosity. The realizable  $k - \varepsilon$  model has been extensively validated for a wide range of flows, including rotating homogenous shear flows, free flows with mixing layers, channel-boundary layer flows, and separated flows. Derived energy equations and details for the realizable  $k - \varepsilon$  model can be found in section 4.3.3 of the ANSYS® Fluent Theory Guide published in 2013.

### 3.5 Boundary Conditions

The boundary conditions used in the CFD model simulated the experimental test chamber at REEL that was built according to the ASTM procedure for capture efficiency. Thus, the air inlet was set to the vent-inlet condition, which refers to ambient air. At the supply air inlet, the CO<sub>2</sub> concentration of the air was initially set to 470 ppm, which is typical for outdoor air, and then it remained constant. As mentioned previously, carbon dioxide (CO<sub>2</sub>) is used as the tracer gas for this study and defined as a mass flow inlet, which is in addition to outdoor air entering the chamber. The relative gas density of CO<sub>2</sub> inside the storage tank is 1.52 kg/m<sup>3</sup>, the mass flow rate of CO<sub>2</sub> gas at different injection rates based on a volumetric flow were calculated using Equation 3.

$$\dot{m} = \rho \times \dot{V} \quad [3]$$

where,  $\dot{m}$  presents the mass flow rate of the tracer gas,  $\rho$  is the density, and  $\dot{V}$  is the volumetric flow rate of the injection rate of CO<sub>2</sub>. The actual calculated mass flow rates of CO<sub>2</sub> injected into the chamber, representing the three different test conditions, are tabulated in Table 3.



Table 3: CO<sub>2</sub> Mass Flow Rate Test Conditions

<b>Volumetric flow rate (l/m)</b>	<b>Calculated mass flow rate (kg/s)</b>
20	$5.1 \times 10^{-3}$
30	$7.6 \times 10^{-3}$
40	$10.1 \times 10^{-3}$

As a final note on CO<sub>2</sub> injection, the tracer gas is designed to be 98% pure carbon dioxide, which is why the concentration of the CO<sub>2</sub> mass flow inlet was initially set to be 980,000 part per million (ppm). With regards to airflow, the air mass flow outlet is a chamber boundary condition that depends on the range-hood fan speed and thus flow, which can be set at any of three 160 CFM, 250 CFM, and 300 CFM, representing three test conditions. In this study, the temperature of the top surface of the emitter plates were maintained at  $160^{\circ}\text{C} \pm 10^{\circ}\text{C}$  continuously during CE tests, according to the ASTM E3087 procedure; hence, the boundary condition for the top surface of two burners were set at a constant wall temperature condition. The aforementioned boundary conditions for the CFD simulations are summarized in Table 4.

Table 4: Boundary Conditions for the CFD Simulations

<b>Location</b>	<b>Boundary conditions type</b>
Chamber ambient air inlet	Inlet vent
CO <sub>2</sub> inlet	Mass flow outlet
Chamber Exhaust	Mass flow outlet
Burners	Wall (surface with fixed temperature)

For the CFD model, the gas inside the test chamber was modeled as a mixture of two major species: air and carbon dioxide, with the air containing oxygen, nitrogen, and water vapor. For all simulations performed for this study, the number of iterations were set to 2,000 and the time scale factor was set to 0.25. With the boundary conditions being completely defined as per earlier discussions, the computational fluid dynamics analyses were conducted with each of the simulations taking approximately 24 hours to process data and complete.

## **CHAPTER 4. VALIDATION OF CFD MODEL USING EXPERIMENTAL CE VALUES**

This chapter describes the validation testing of the computational fluid dynamics (CFD) model by comparing CO<sub>2</sub> concentration and capture efficiency (CE) outputs from the CFD simulations with the experimental results taken on the REEL test facility. The results for CO<sub>2</sub> concentration measurements at the three aforementioned locations and the resulting CE values for all three cases, representing three different operating speeds and their respective injection flow rates, are tabulated for each method in two tables, namely experimental and CFD. Finally, the experimental and CFD results are compared to validate the ability of the model to provide accurate CE results that are consistent with guidelines in ASTM-E3087.

### **4.1 Experimental Results Summary**

Multiple experiments were performed on the Venmar range hood at three different operating speeds and at the three respective injection rates using the actual CE test facility at REEL, following the procedures specified in ASTM-E3087. These experimental results are presented in Table 5 with the left two columns of the table presenting the operating speeds and injection rates of the CO<sub>2</sub> tracer gas used in the CE tests. The three range-hood speed settings were 160 CFM (low speed), 250 CFM (medium speed), and 300 CFM (high speed); and the three tested injection rates for these speeds were 20 l/m, 30 l/m, and 40 l/m respectively. As previously mentioned, the CO<sub>2</sub> concentrations at the three locations, namely at the chamber inlet, in the chamber volume, and at the exhaust, were experimentally measured using CO<sub>2</sub> sensors. Table 5 also includes the CO<sub>2</sub> concentration

measurements at these three locations for each speed and most importantly the calculated range-hood capture efficiencies (CE) again for all three speeds. It should be noted again that the Table 5 experimental data are for tests performed on the Venmar Inspira IU600ES30BL range-hood unit, following guidelines in ASTM-E3087. Also of note, the CE values shown in Table 5 are calculated from CO<sub>2</sub> concentration measurements using Equation 1. After the next subsection, this experimental Table 5 data will be used for the CFD model validation.

Table 5: Experimental Test Results consisting of CO<sub>2</sub> Concentrations and CE Values

Range Hood Speed (CFM)	Injection Rate (l/m)	CO <sub>2</sub> Concentrations			CE (%)
		Inlet (ppm)	Chamber (ppm)	Exhaust (ppm)	
160	20	488	2180	4612	59.0
250	30	510	1708	4870	72.5
300	40	498	796	5055	93.5

Several observations can be made from a study of the data in Table 5. For example, CE values are shown to increase with increased fan speeds. With regard to CO<sub>2</sub> concentrations, the values are relatively unchanged at the inlet and exhaust as the fan speed is increased; however, the chamber CO<sub>2</sub> concentration, which represents the contaminants inhaled by the indoor space occupants, decreases considerably with increases in fan speed.

## 4.2 CFD Numerical Results Summary

Using the same test conditions described previously for the experimental study, three CFD simulations were performed, corresponding to each of the three testing combinations of fan speed and injection rate. Presented in Table 6 are the CFD simulation-predicted CO<sub>2</sub> concentrations at the three aforementioned locations and the calculated CE results, again using Equation 1, for all three fan speed cases.

Table 6: CFD Predicted Values of CO<sub>2</sub> Concentrations and CE Values

Range Hood Speed (CFM)	Injection Rate (l/m)	CO <sub>2</sub> Concentrations			CE (%)
		Inlet (ppm)	Chamber (ppm)	Exhaust (ppm)	
160	20	470	2370	5150	59.4
250	30	470	1620	4980	74.5
300	40	470	775	5225	93.6

The Table 6 results for predicted CO<sub>2</sub> concentrations and capture efficiencies follow the same trends previously discussed for Table 5.

## 4.3 Validation of The CFD Simulation Model Using Experimental Data

The goal of this study is to develop an accurate CFD simulation model and then use this model to evaluate the effects of chamber geometry and dimensions on capture efficiency (CE). With this goal in mind, it is important to validate the model as being accurate, which can only be achieved by showing good agreement between the simulation results and the experimental data. As a first step in this validation, the percentage difference between CE values measured experimentally and those predicted by the CFD simulations were calculated using Equation 4 as follows.

$$\text{Percentage Difference (\%)} = \frac{CE_{CFD} - CE_{Experimental}}{CE_{Experimental}} \times 100 \quad [4]$$

The CE comparison between the CFD predicted results and the experimental data results are summarized and tabulated in Table 7.

Table 7: Percentage Difference Between CFD Predicted Values and Experimental Data

<b>Range Hood Speed (CFM)</b>	<b>Injection Rate (l/m)</b>	<b>Experimental Capture Efficiency (%)</b>	<b>CFD Predicted Capture Efficiency (%)</b>	<b>Percentage Difference From Eq. 4 (%)</b>
160	20	59.0	59.4	0.73
250	30	72.5	74.5	2.73
300	40	93.5	93.6	0.14

Furthermore, the CE values in Table 7 for the two methods, simulated and experimental, are plotted for the three fan speeds in Figure 9, which provides an additional comparison.

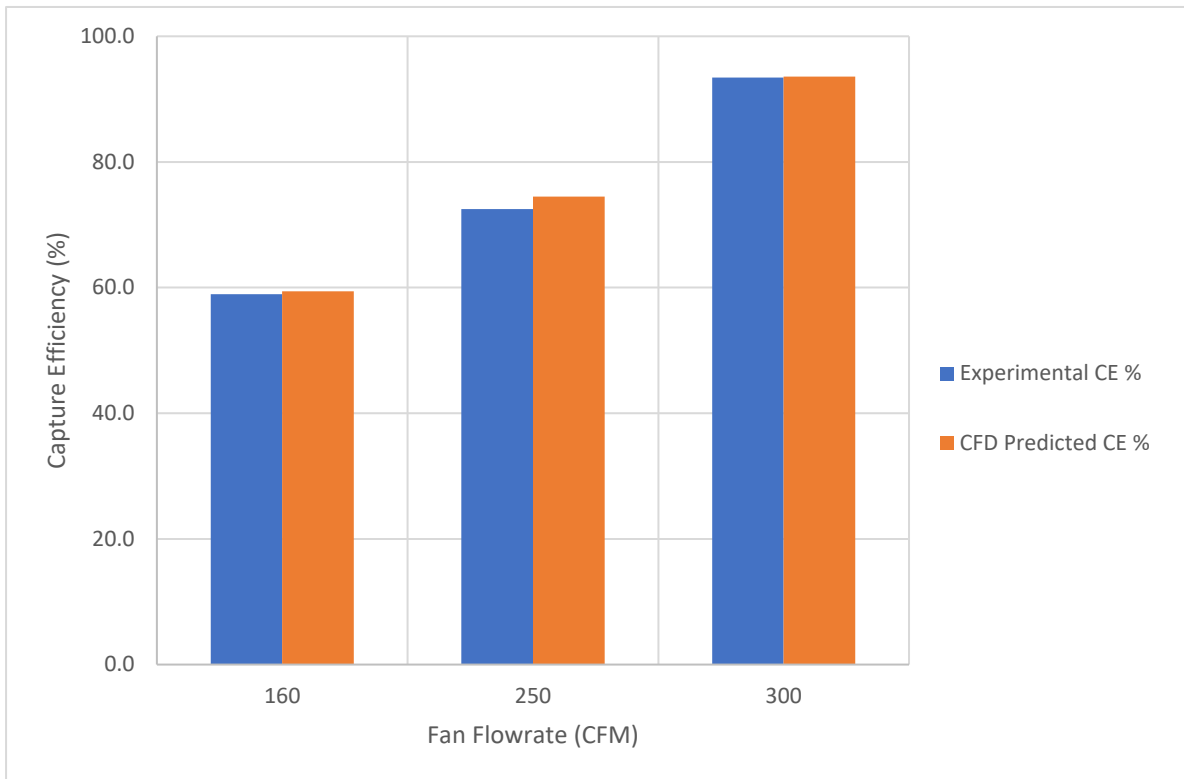


Figure 9: CFD Simulatiopn and Experimentally Measured Capture Efficiency Comparison

From the Table 7 tabulations and the Figure 9 plot one can observe that the\ CFD simulation values for all three cases are similar to the experimental CE measurements for the low, medium, and high fan speeds with differences being 0.73%, 2.73%, and 0.14%, respectively. These results show that the percentage differences across all three exhaust flow rates are below 3% with the maximum difference being 2.73% at the range-hood operating speed of 250 CFM with an injection rate of 30 l/m and a minimum percentage

difference of 0.14% at the high operating speed of 300 CFM with an injection rate of 40 l/m. The remaining percentage difference for the low fan speed is still below 1%. The above results validate the ability of CFD simulation model to predict CE values that are consistent with ASTM-E3087 and, most importantly, confirming that the CFD model can be used as a tool for analyzing and evaluating CE methodologies and test facilities.

Additional insight into difference between simulated results in Table 6 and the experimental results in Table 5 can be gained by comparing CO<sub>2</sub> concentration results (ppm) at the three CO<sub>2</sub> sensor measurement locations for the three fan speeds and injection rates. Table 8 tabulates and compares the ppm values of CO<sub>2</sub> concentration at each location, along with their percentage difference using a relationship similar to Equation 4 for CE. This new Table 8 is essentially a combining of tabulations in Table 5 and 6.

Table 8: Percentage Difference Between CFD Predicted Values and Experimental Data

Range Hood Speed and Injection Rate	CO <sub>2</sub> Concentrations								
	Inlet			Chamber			Exhaust		
	CFD (ppm)	Exp. (ppm)	(%) Dif.	CFD (ppm)	Exp. (ppm)	(%) Dif.	CFD (ppm)	Exp. (ppm)	(%) Dif.
Low	470	488	3.69	2370	2180	8.72	5150	4612	11.7
Medium	470	510	7.84	1620	1708	5.15	4980	4870	2.26
High	470	498	5.62	775	796	2.64	5225	5055	3.36



The agreement between simulated and experimental concentrations are similar for all locations with percentage differences being a minimum of 2.26% and maximum of 11.7%. If the percentage differences are averaged at each location, then one finds 5.7%, 5.5%, and 5.8% at the inlet, chamber, and exhaust location, respectively.

## **CHAPTER 5. CFM MODEL ANALYSIS OF CO<sub>2</sub> CONCENTRATION DISTRIBUTIONS AND SAMPLING LOCATIONS**

After validating the computational fluid dynamics (CFD) simulation model, the CO<sub>2</sub> concentration distribution inside the chamber was determined and then analyzed. The goal of this evaluation is to find the optimum sampling position for the chamber CO<sub>2</sub> concentration, which is one of three concentrations used to calculate the range-hood capture efficiency (CE).

### **5.1 Overview**

The purpose of this analysis was to use the CFD simulation model to predict CO<sub>2</sub> concentration values at different locations inside the chamber, including the measurement location presently specified in ASTM-E3087. It should be noted that experimentally measuring CO<sub>2</sub> concentrations using sensors throughout the CE chamber is difficult, if not impossible, because of the large number of sensors needed. In contrast, the CFD simulation model is an ideal tool for accomplishing this task because the chamber CO<sub>2</sub> distribution is part of the model output.

After finding CO<sub>2</sub> concentrations at select locations using the CFD model, then the results can be plugged into Equation 1 to find chamber CE values. Next, these CE values are compared to determine the effects that the CO<sub>2</sub> sensor locations inside the chamber might have on CE measurements. It is important to note when determining CE values that the sensors at the inlet and exhaust of the test facility are fixed, meaning unchanged, which also means that the CO<sub>2</sub> concentrations are fixed. Again, only the CO<sub>2</sub> sensor location in the chamber, along with its CO<sub>2</sub> concentration, factors into the investigation of CE effects

## 5.2 Methodology

In addition to the original CO<sub>2</sub> sampling location specified in ASTM-E3087 for measuring the chamber CO<sub>2</sub> concentration, three additional CO<sub>2</sub> concentration measurement locations were defined and added to the CFD simulation model for analysis. These locations were sensor 1 at the left wall, sensor 2 at the front door, and sensor 3 at the right wall. These three additional sampling locations, namely 1 through 3, were assumed to be at the same height as the original sensor location chamber, which is 5.25 feet (1.6 m) above the ground. Figure 10 depicts a schematic of the control volume of the CFD model with the three additional sampling locations being shown in red along with the original location in blue.

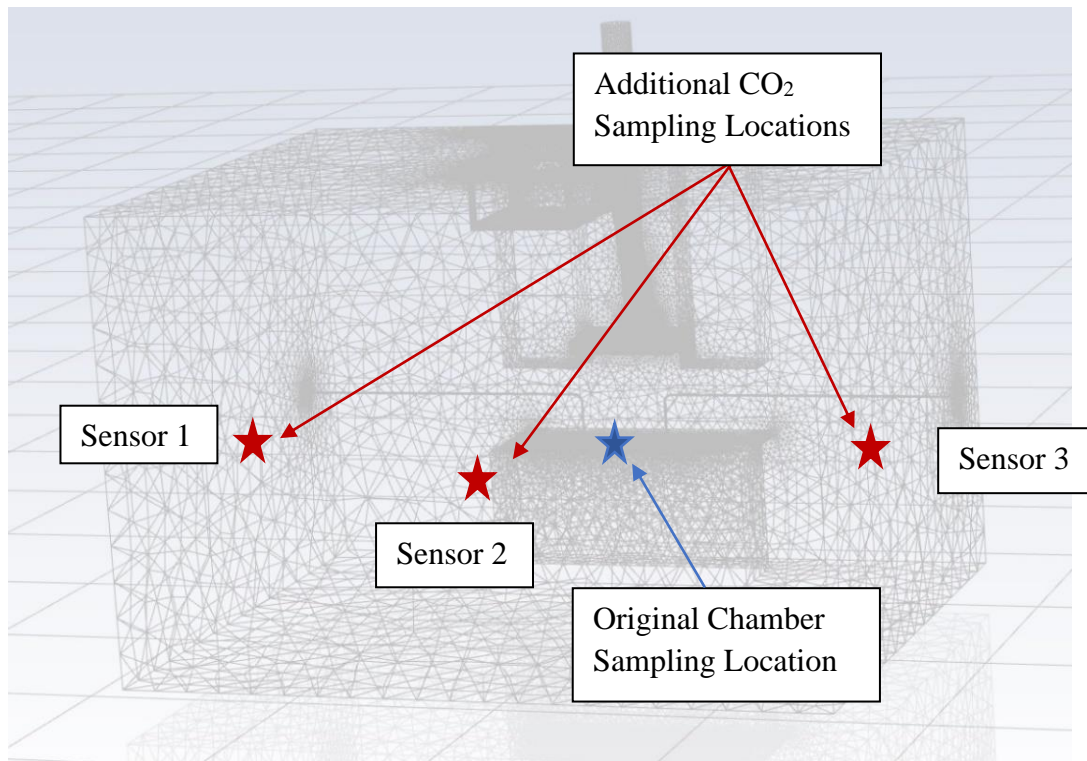


Figure 10: A Schematic of the Volume Vontrol of the CFD Model showing the Three Additional CO<sub>2</sub> Concentration Measurement Locations along with the Original Chamber Location

### 5.3 Summary of Results and Discussion

The CO<sub>2</sub> concentrations taken from the CFD simulations for the original location and the three new sampling locations are summarized and compared in Table 9. Also shown in Table 9 are the calculated capture efficiencies (CE).

Table 9: Comparison Summary of CO<sub>2</sub> Concentrations and CE at Four Location based on CFD Simulations

Range Hood Speed and Injection Rate	CO <sub>2</sub> Concentrations and Calculated CE Values							
	Chamber Location		Left Wall Location		Front Door Location		Right Wall Location	
	Chamber (ppm)	CE (%)	Sensor 1 (ppm)	CE (%)	Sensor 2 (ppm)	CE (%)	Sensor 3 (ppm)	CE (%)
Low	2370	59.4	2450	57.7	1750	72.6	2475	57.2
Medium	1620	74.5	1775	71.1	1525	76.6	1710	72.5
High	775	93.6	800	93.1	680	95.6	780	93.5

The calculated CE values for the four locations, namely sensor 1 (left wall), sensor 2 (front door), sensor 3 (right wall), and original chamber location specified in ASTM-E3087, were then plotted for direct comparison in Figure 11.

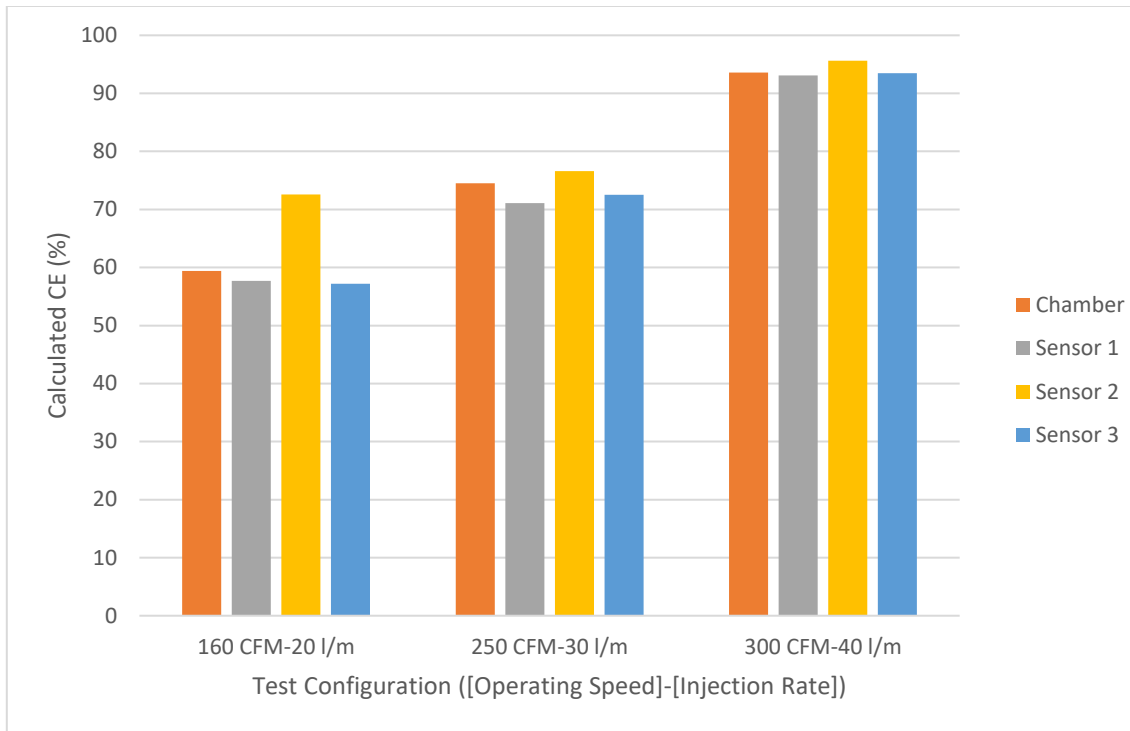


Figure 11: Comparison of Calculated CE Results at the Four Different Sampling Locations

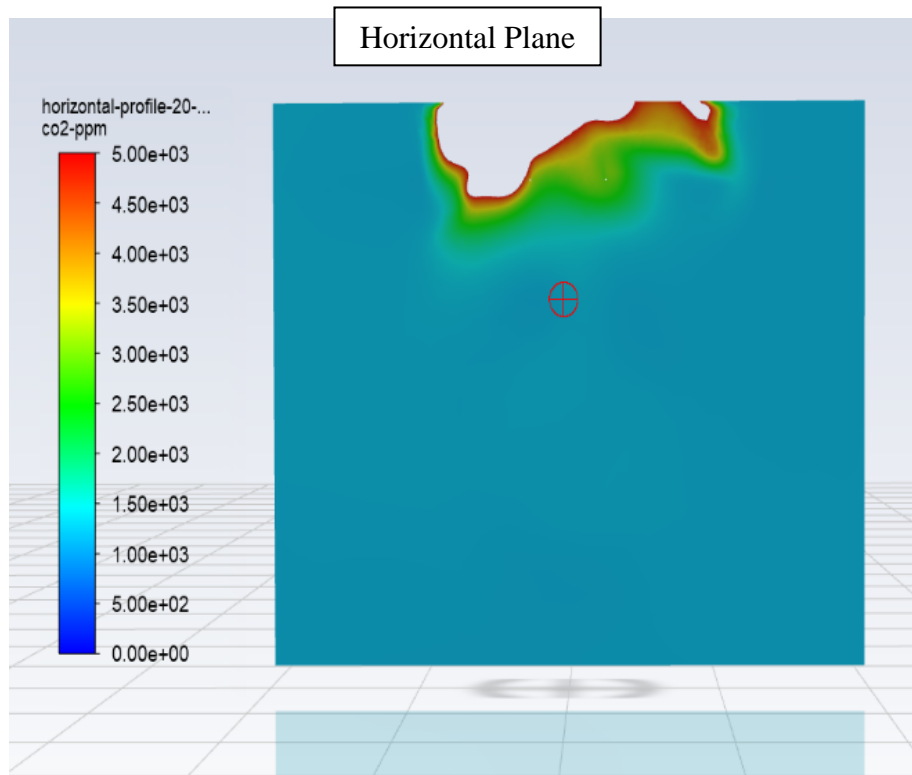
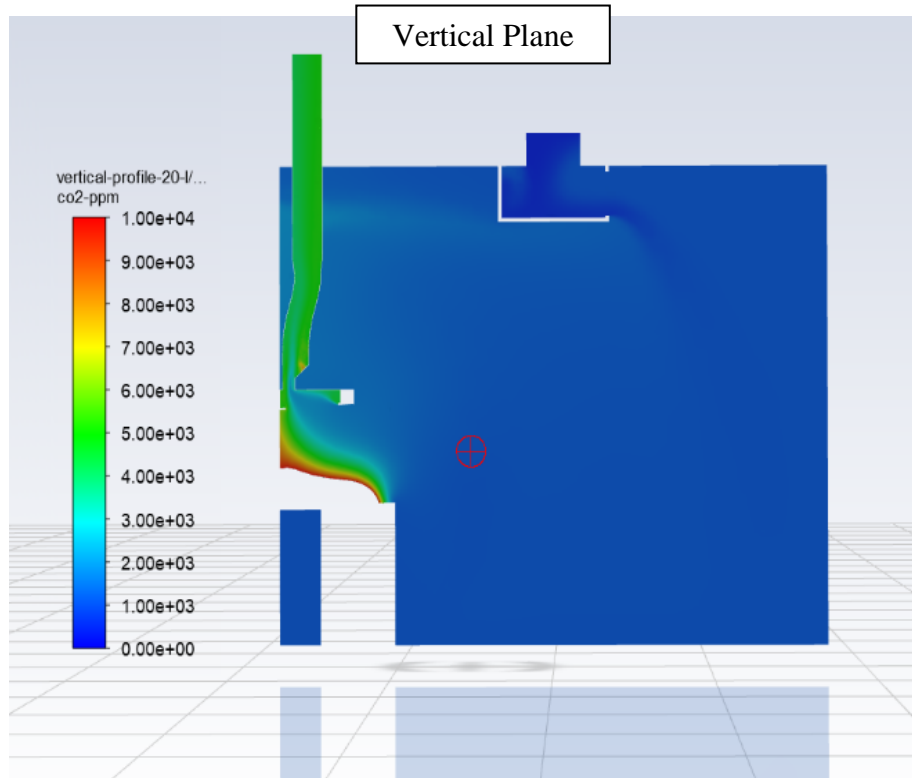
The results tabulated in Table 9 and plotted in Figure 11 appear to show that the calculated CE values for each fan speed appears to be somewhat independent of measurement location, with fan speed certainly having a much larger effect than sampling location. An additional analysis further quantifies the CE difference with location. Specially, this location comparison of CE is based on using CE data in Table 10 to determine the percent CE difference between each new sensor location and the original chamber location, which is treated as a reference. The results of this percent CE difference calculation are tabulated in Table 10 for each fan speed, with their respective injection rates.

Table 10: Comparison of Calculated Capture Efficiency (CE) at Sampling Locations by using the Chamber Location CE as Specified in ASTM-E3087 as a Reference

<b>Range Hood Speed (CFM)</b>	<b>Injection Rate (l/m)</b>	<b>Sensor Locations</b>	<b>Capture Efficiency (%)</b>	<b>Absolute Percentage Difference from Reference CE (%)</b>
160	20	Sensor 1	57.7	2.9
		Sensor 2	72.6	22.3
		Sensor 3	57.2	3.8
250	30	Sensor 1	71.1	4.6
		Sensor 2	76.6	2.8
		Sensor 3	72.5	2.7
300	40	Sensor 1	93.1	0.6
		Sensor 2	95.6	2.1
		Sensor 3	93.5	0.1

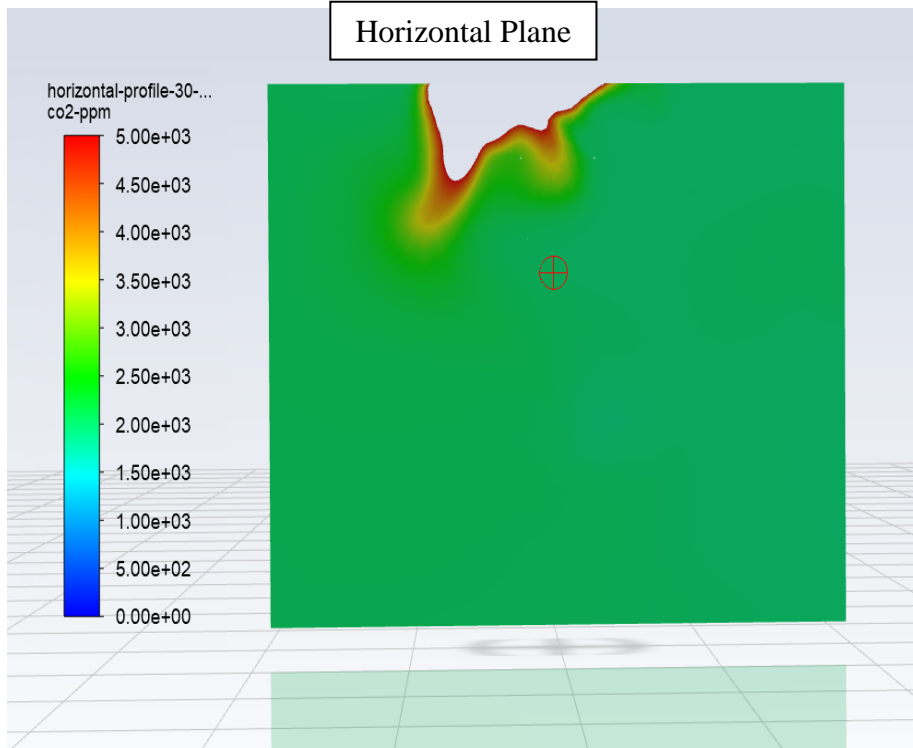
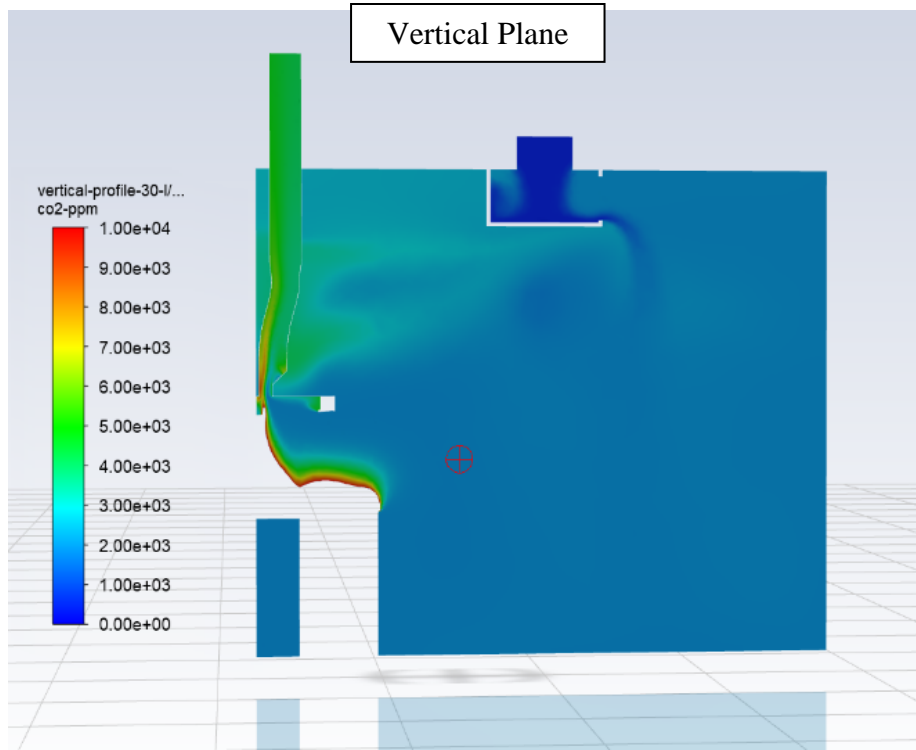
A number of interesting observations can be made by analyzing the tabulations in Table 10, which are the percentage differences between CE values at the three new locations and the chamber reference values specified in the standard. For example, the CO<sub>2</sub> concentrations for sensor 2 located at the door of the chamber were lowest, which in turn resulted in the highest calculated CE. In fact, at a low fan speed setting of 160 CFM with a CO<sub>2</sub> injection rate 20 l/m, the CO<sub>2</sub> concentration decreases about 26.6% below the chamber reference concentration, which resulted in the highest calculated CE with a percentage difference from the reference value of 22.3%. For simulations at the other two speeds, the CO<sub>2</sub> concentrations at the sensor 2 location were also found to be higher, but the CE results were only slightly higher, so that the CE results were higher by only 2% to 3%. It should be noted that, the chamber concentrations at the sampling location specified in ASTM-E3087 were higher than the concentrations measured at sensor 1 and 3 locations for all three fan speed cases by less than 5%.

In order to aid the visualization of the results, Figure 12 presents CFD generated contours of steady-state CO<sub>2</sub> concentration distributions along the vertical planes (top side plot) and the horizontal planes (bottom side plot) for the three fan speeds and injection rates. Specially, Figure 12.a is for the lowest fan speed of 160 CFM and injection rate of 20 l/m, Figure 12.b. is the medium for speed of 250 CFM and injection rate of 30 l/m, and finally Figure 12.c is the highest fan speed of 300 CFM and injection rate of 40 l/m.

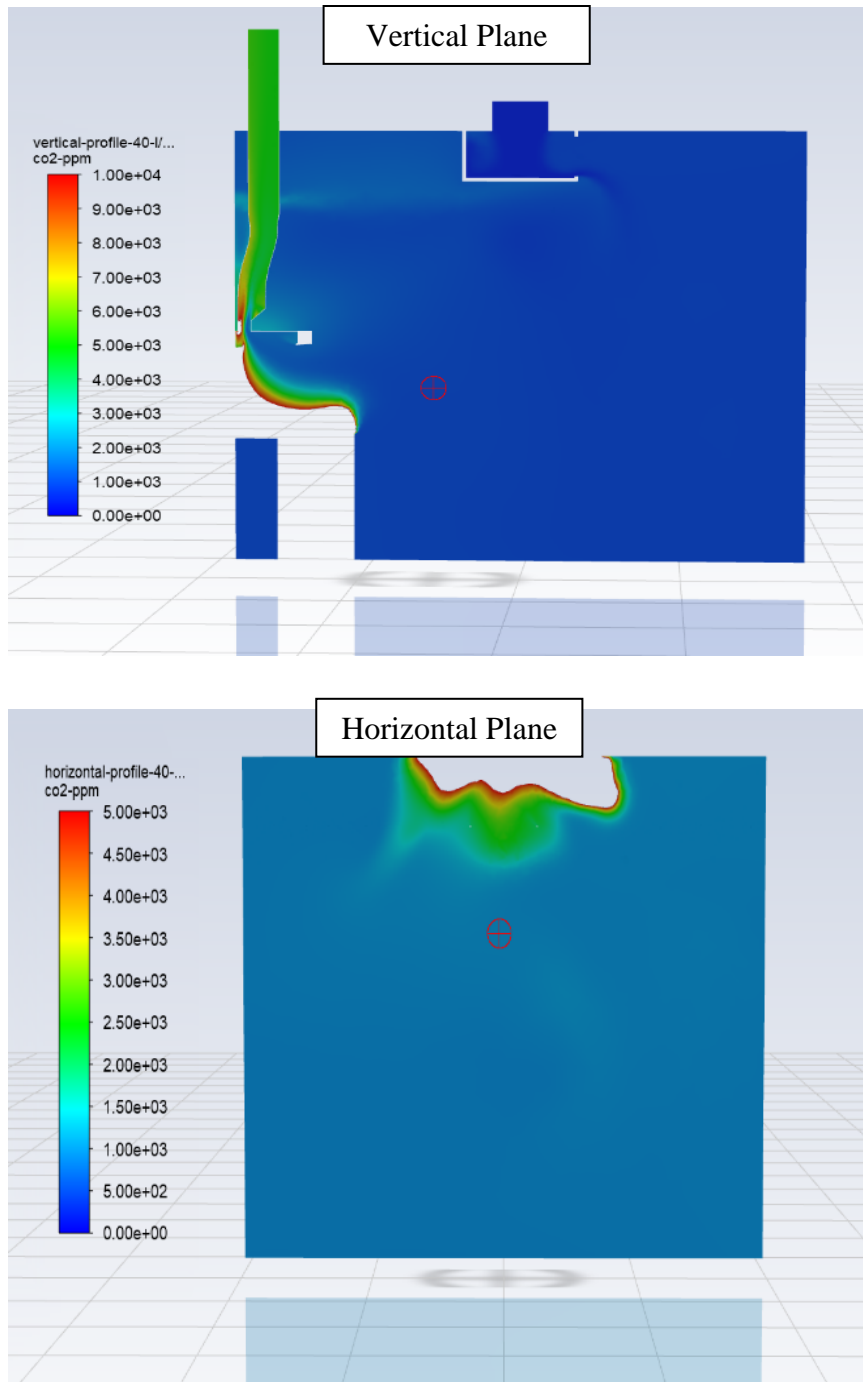


a) Lowest Air Flowrate of 160 CFM and CO<sub>2</sub> Injection Rate of 20 l/m





b) Medium Air Flowrate of 250 CFM and CO<sub>2</sub> Injection Rate of 30 l/m



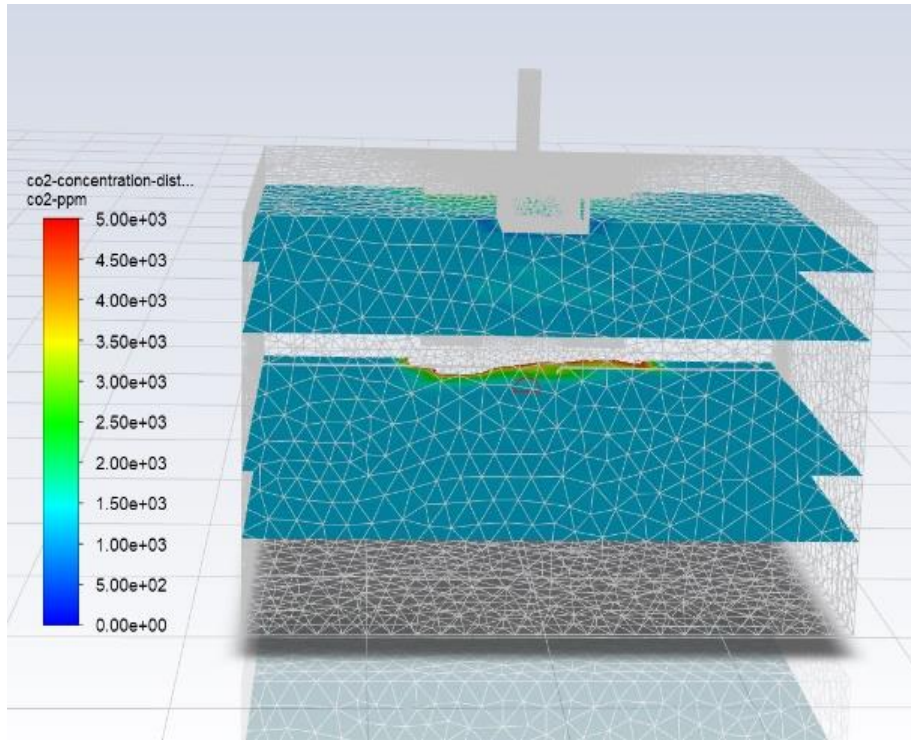
c) Highest air flowrate of 300 CFM and CO<sub>2</sub> injection rate of 40 l/m

Figure 12: Distributions of Steady-state CO<sub>2</sub> Concentration on the Vertical Cross-sectional Planes (top side plot) and the Horizontal Cross-sectional Planes (bottom side plot) for Three Simulations

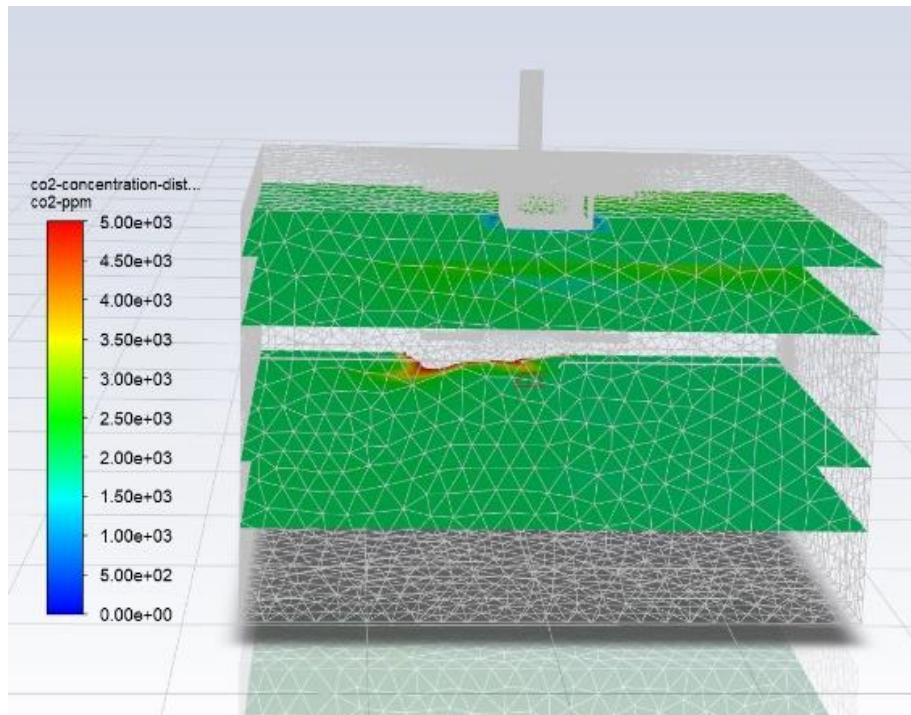
As shown in Figure 12, CO<sub>2</sub> concentration stratifications appear to increase as one moves closer to the countertop and the range hood, which is an indication of the variance of CO<sub>2</sub> concentration in the mixture inside the chamber. Figure 12 also shows that the convective flow phenomena cause the mixture gas to travel upward so as to accumulate by the range hood located above the heat sources, which in turn leads to significant vertical variations in concentration below the range hood. The differences between the concentrations at the chamber sampling location and the area around the heat sources are high, with concentration varying from 3000 ppm to 5000 ppm.

It can also be observed that at the sampling location specified in ASTM-E3087, stratifications still exist and show some variance; however, the CO<sub>2</sub> concentration distributions are more uniform with less of a gradient than at other locations, which may be due to well-mixed airflow conditions being achieved away from the walls and door. By moving the sensor further from the countertop and closer to the door of the chamber, the CO<sub>2</sub> concentration appears to be reduced, probably due to this location being further from the CO<sub>2</sub> emitter source at the stovetop and because of the direction of the supply air from the inlet, this concentration dip near the door would suggest that this location may not be representation of the chamber as a whole.

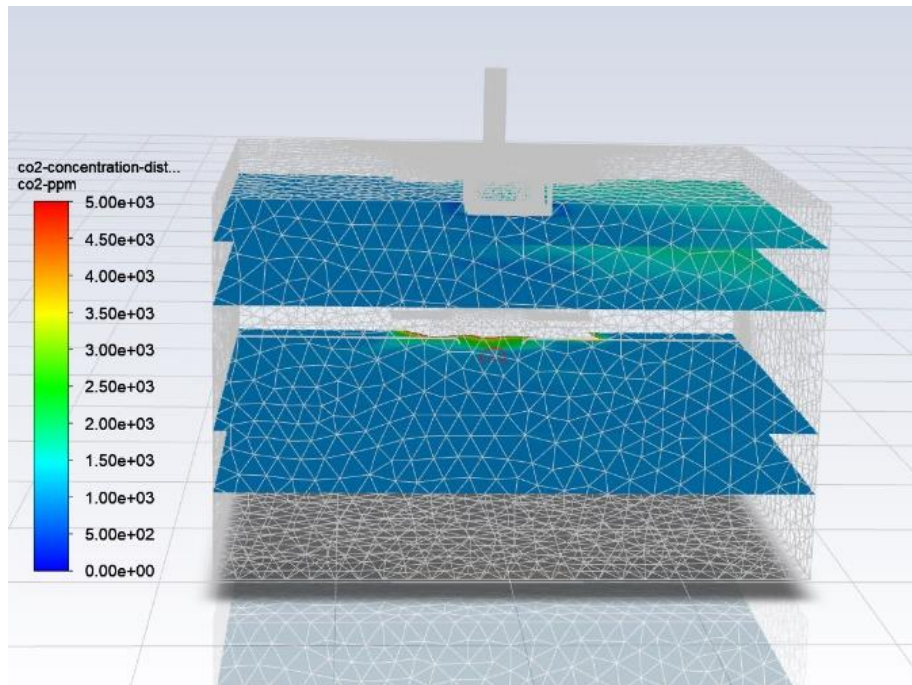
The following Figure 13 presents the CO<sub>2</sub> concentration profiles along horizontal cross-sectional planes at different heights above the floor 3.6 feet (1.1 m) , 5.3 feet (1.6 m), 8.6 feet (2.6 m), and 10.3 feet (3.1 m) for the 3 test combinations of flow rates and injection rates.



a) At 160 CFM – 20 l/m



b) At 250 CFM – 30 l/m



c) At 300 CFM – 40 l/m

Figure 13: Distributions of Steady-state CO<sub>2</sub> Concentrations on Horizontal Cross-sectional Planes at Four Different Heights

It can be visually observed from Figure 13 that the CO<sub>2</sub> concentration varies with height inside the test chamber, meaning that there are differences between the concentrations just above the floor and the area close to the ceiling of the chamber. The concentrations of CO<sub>2</sub> are higher at the top plane compared to the bottom plane. In addition, Figure 13 shows that the concentration distributions are less uniform on the top planes while the plane at the height of 5.3 feet (1.6 m) appears to have the most uniform CO<sub>2</sub> concentration distribution, signifying regions inside the chamber where the mixture is well mixed, which also corresponds to a region with CO<sub>2</sub> concentration that may be representation of the chamber as a whole.

The results of the CFD simulations would appear to verify that the tracer gas sampling should be located on the centerline of the test chamber and installed 5.3 feet (1.6m) above the ground, and possibly 1.7 feet (0.5 m) away from the countertop table, following the procedures outlined in ASTM-E3087. This location corresponds to a region that has CO<sub>2</sub> concentrations that are most representative of the chamber as a whole, meaning a CO<sub>2</sub> concentration sensor placed here contributes to the most accurate CE value inside the chamber.

As a final note, there are notable differences in CO<sub>2</sub> concentration measurement when moving the sampling too far away from the countertop table, using these locations which could affect the accuracy of measuring the capture efficiency of the domestic range-hoods. As mentioned previously, the calculated capture efficiencies are higher in the door chamber region near sensor 2; however, this location was observed to have a less uniform CO<sub>2</sub> distribution so that it does not indicate well-mixed air or CE results accuracy.

To summarize, the differences in CE results obtained from this CO<sub>2</sub> concentration distribution study of different locations shows that the current chamber sampling location as specified in ASTM-E3087 corresponds to the most uniform of CO<sub>2</sub> distributions. This result thus confirms that the original chamber sampling location is the best “chamber” location for placing the CO<sub>2</sub> sensor for CE testing.

## **CHAPTER 6. IMPACT OF CHAMBER VOLUME ON CAPTURE EFFICIENCY MEASUREMENTS**

After completing formulation of the computational fluid dynamics (CFD) model and the validation step, an investigation was launched to use the model to determine the effect of the test chamber volume on range-hood capture efficiency. This study goal to identify the correlation between the capture efficiency of range-hoods and the volume of the CE test chamber is important for designing and selecting the appropriate chamber size and for comparing CE results from different organizations with different size facilities. Using the CFD simulation model approach to evaluate the relationship between capture efficiency and chamber volume takes less time and effort than physically building multiple chambers of different sizes and then performing CE tests on each.

First, the model description and dimensions used in simulations are listed and explained. Then the results are summarized and compared to determine the sensitivity of capture efficiency results to changes to the volume of the chamber.

### **6.1 Background and Methodology**

Other than the REEL test facility chamber reported herein, only one other CE test facility, which is located at the Lawrence Berkley National Laboratory (LBNL), has been built and operated to experimentally measure the capture efficiency of range-hoods following the guidelines presented in ASTM-E3087. Unexpectantly, the CE tests results that were reported by LBNL using their test facility are higher than those measured by REEL. The two labs used the same standard method outlined in ASTM-E3087, and the experiments were performed on the same range-hood fan samples at their respective fan

speed settings. The one notable difference between these series of CE tests from different facility is that they were performed on two chambers that have different dimensions and volumes. For example, the size of the LBNL chamber is reported to be 15.1 feet (4.6 m) wide by 7.5 feet (2.3 m) deep and 7.9 feet (2.4 m) tall while the size of the REEL test chamber located at RELLIS is 16.4 feet (5 m) wide by 13.1 feet (4 m) deep and 9.8 feet (3 m) tall, with both sizes being as tabulated and compared in Table 11. The total volume of the LBNL chamber is  $896.7 \text{ ft}^3$  ( $25.4 \text{ m}^3$ ) while the volume of the REEL chamber was found to be  $2118.9 \text{ ft}^3$  ( $60.0 \text{ m}^3$ ), making the REEL chamber about 2.36 times larger than the volume of the LBNL chamber, again tabulated and compared in Table 11. It should be noted that the minimum dimensions of a test chamber as specified in ASTM-E3087 are 11.5 feet (3.5 m) wide by 8.2 feet (2.5 m) deep and 7.9 feet (2.4 m) tall, which produce a volume of  $741.6 \text{ ft}^3$  ( $21.0 \text{ m}^3$ ), making the REEL chamber about 2.86 times larger than the standard minimum volume.

In addition to the above three chamber sizes, a fourth chamber size was considered in this study. This chamber size and volume is based on reducing the depth of the REEL chamber from 13.1 feet (4.0 m) to 8.2 feet (2.5 m) with this new depth being equivalent to the minimum-dimensions depth in the standard, while keeping all other dimensions unchanged, as shown in Table 11. The effect on volume is that the REEL chamber as constructed is 1.6 times larger than the aforementioned chamber. All dimensions and sizes of the four chambers are summarized and compared in Table 11.



Table 11: Comparison of Dimensions and Volumes for Four Chambers

Chamber Description	Chamber Dimensions			Chamber Volume- $ft^3 (m^3)$	Percentage Volume Reduction %	Reference Chamber Ratio $\left(\frac{V_{REEL}}{V}\right)$
	Width- $ft (m)$	Depth- $ft (m)$	Height- $ft (m)$			
<b>REEL Chamber</b>	16.4 (5.0)	13.1 (4.0)	9.8 (3.0)	2118.9 (60.0)	0	1
<b>Depth-Reduced Chamber</b>	16.4 (5.0)	8.2 (2.5)	9.8 (3.0)	1324.3 (37.5)	37.5	1.60
<b>LBNL Chamber</b>	15.1 (4.6)	7.5 (2.3)	7.9 (2.4)	896.7 (25.4)	57.8	2.36
<b>ASTM Minimum Dimensions Chamber</b>	11.5 (3.5)	8.2 (2.5)	7.9 (2.4)	741.6 (21.0)	65.0	2.86

Based on the above discussion, a series of CFD simulations was conducted for four different test chambers listed in Table 11, including the actual REEL test chamber, the LBNL test chamber, the standard minimum chamber specified in ASTM-E3087, and finally, a chamber similar to the REEL chamber but with a depth reduction as shown in

Table 11. As discussed previously, this new chamber size is based on keeping the REEL chamber width and height size unchanged but then reducing the chamber depth to a standard minimum-dimension chamber depth values, which results in a 37.5% volume reduction.

The chamber volumes comparison is further showcased in a volume bar chart shown in Figure 14 which provides a thorough visualization of the differences between the chamber volumes.

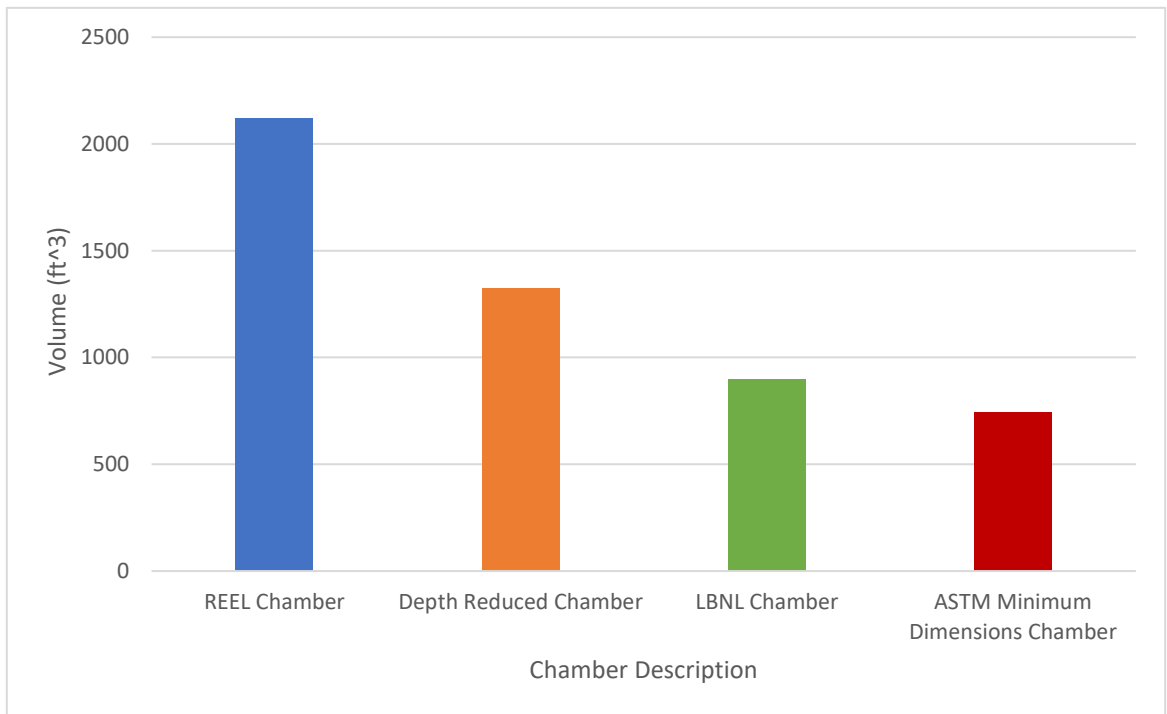


Figure 14: Bar-chart Comparison of the Total Volume of the Four Chambers

The output of these CFD simulations is capture efficiency (CE) for each of the four different chamber volumes at the same fan operating speed of 160 CFM and at CO<sub>2</sub> injection rate of 20 l/m. Additionally, the simulations were performed with 2000 iterations

using a 0.25 second time-step setting while the mesh configuration for the four models was well defined by approximately 9.0 million elements.

It should be noted that the REEL chamber CFD simulation model CE results used in this volume study were taken from previous sections where it was used to validate the CFD approach. In contrast, it was necessary to formulate and run new CFD simulations to obtain CE results for the depth-reduced chamber, the LBNL chamber, and the ASTM minimum-dimension chamber.

## 6.2 Summary of Results and Discussion

Using the same settings and conditions as described previously, four CFD simulations were performed on the four different chamber volumes. The CO<sub>2</sub> concentration distributions and the capture efficiency (CE) results from these simulations are summarized in Table 12. It is important to note that the CE values are found from CO<sub>2</sub> concentrations using the following relationship.

$$CE = \frac{C_{exhaust} - C_{chamber}}{C_{exhaust} - C_{ambient}} \quad [1]$$

Table 12: Summary of CO<sub>2</sub> Concentrations and Calculated CE Values for Four Different Chamber Sizes using the CFD Simulation Model

Model Description	CO <sub>2</sub> Concentration			CE (%)	Percentage Difference Referenced to REEL Value (%)
	Inlet (ppm)	Chamber (ppm)	Exhaust (ppm)		
<b>REEL Chamber</b>	470	2370	5150	59.4	0
<b>Depth-Reduced Chamber</b>	470	2120	5175	64.9	9.3
<b>LBNL Chamber</b>	470	1825	5050	70.4	18.5
<b>ASTM Minimum-Dimension Chamber</b>	470	1575	5015	75.7	27.4

From the Table 12 results, the calculated CE for the three simulation models, namely depth-reduced chamber, LBNL chamber, and ASTM minimum-dimension chamber, are higher than the CE value using the actual REEL chamber model, which has the same chamber dimensions as the installed test facility. A direct comparison of CO<sub>2</sub> concentrations at the three relevant locations for the four chamber volumes are presented in Figure 15. Similarly, the calculated range-hood capture efficiencies calculated from the concentrations using Equation 1 are shown in Figure 16 for the four volumes.

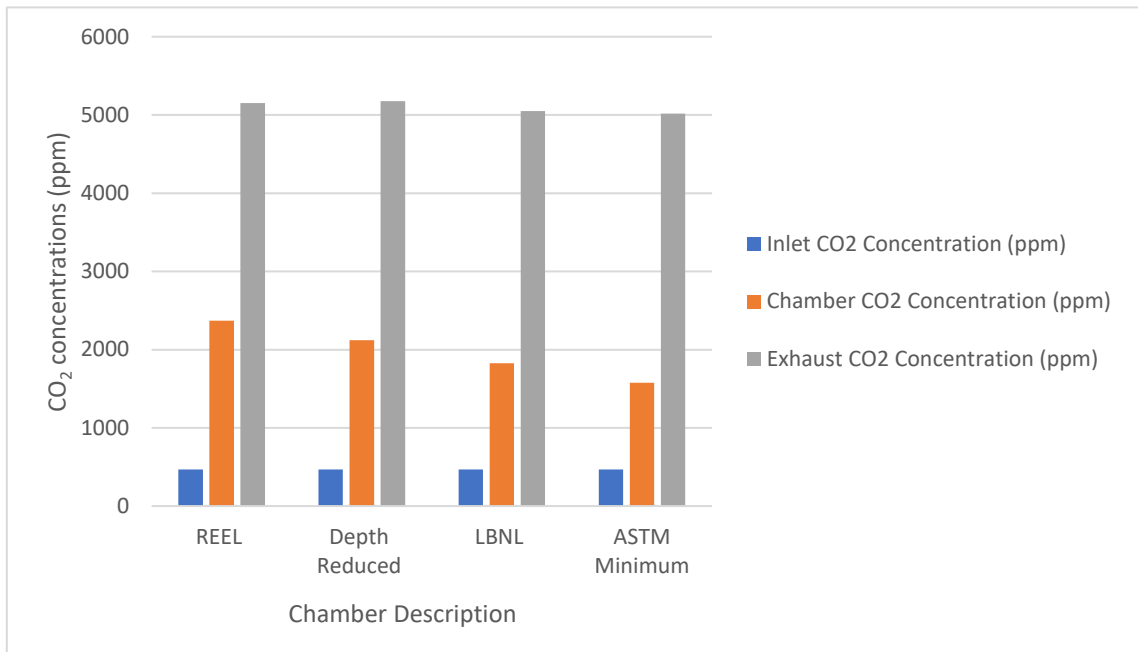


Figure 15: Comparison of CO<sub>2</sub> Concentrations at three Standard Specified Sampling Locations for the Four Chambers Volumes

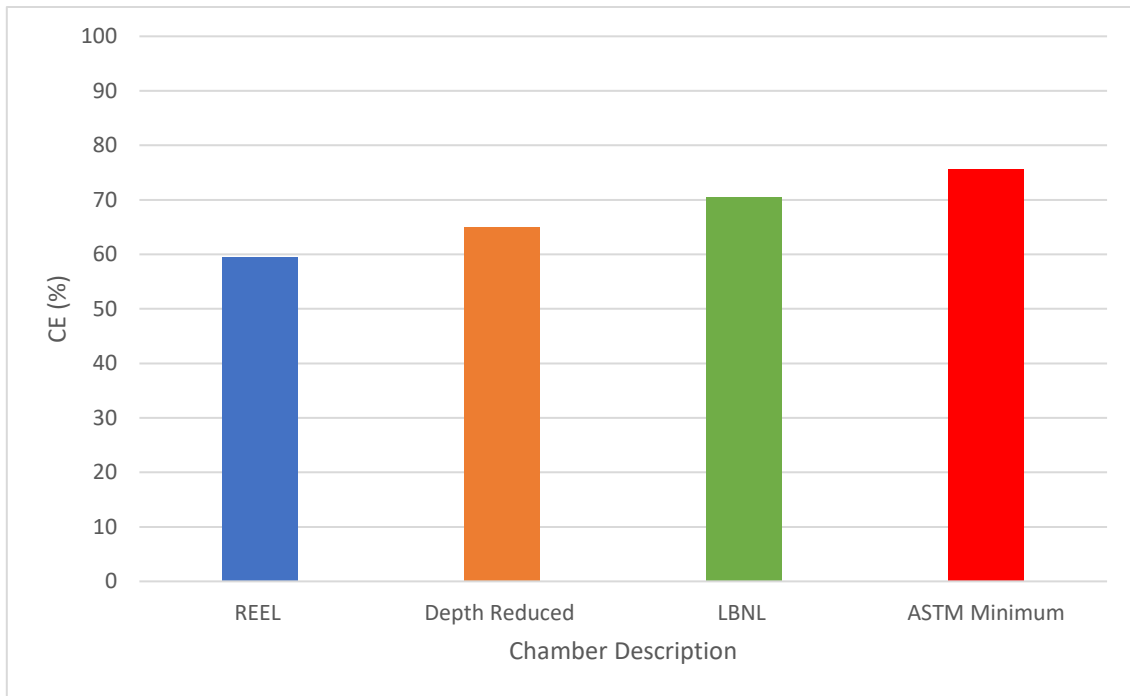


Figure 16: Comparison of Calculated Range-hood CE Values for the Four Chamber Volumes

A number of interesting observations can be made from an analysis of the CO<sub>2</sub> concentration results plotted in Figure 15 and tabulated in Table 12. In contrast to the inlet and exhaust CO<sub>2</sub> concentrations that are independent of volume, the ppm CO<sub>2</sub> concentration of the air within the chamber becomes significantly lower as the volume of the chamber is reduced. In fact, the concentration in the chamber decreases about 35% from the largest to smallest value, meaning the chamber concentration is markedly affected by volume, which undoubtedly effects the final capture efficiency (CE) values. In fact, the percentage difference from the highest to the lowest CE value is 27.4%. Also of note, the CO<sub>2</sub> concentration in the air at the inlet to the four different chambers, which is representation of a typical outdoor or ambient value, is set to be a fixed 470 ppm based on this being a boundary condition of the CFD model. The CO<sub>2</sub> concentrations in the chamber exhaust ducting change only slightly with respect to the decrease in the volume of the chamber; with the difference between the highest and lowest values of CE being about 3%, which is certainly does not account for the 27.4% difference between the highest and lowest CE values.

The relationship between chamber volume and the capture efficiency (CE) result can be found by analyzing the CE data in Figure 16 and Table 12. The CFD calculated range-hood CE for the minimum dimensions chamber specified in ASTM-E3087 was found to be about 27.4% higher compared to the CE value for the current REEL chamber model. The depth-reduced chamber model and LBNL chamber model also produced results higher than the current REEL chamber model by 9.3% and 18.5% respectively. It would appear that the chamber volume effects the capture efficiency results, and to further

quantify this effect, capture efficiency values are plotted with respect to chamber volume in Figure 17 for each of the four chambers.

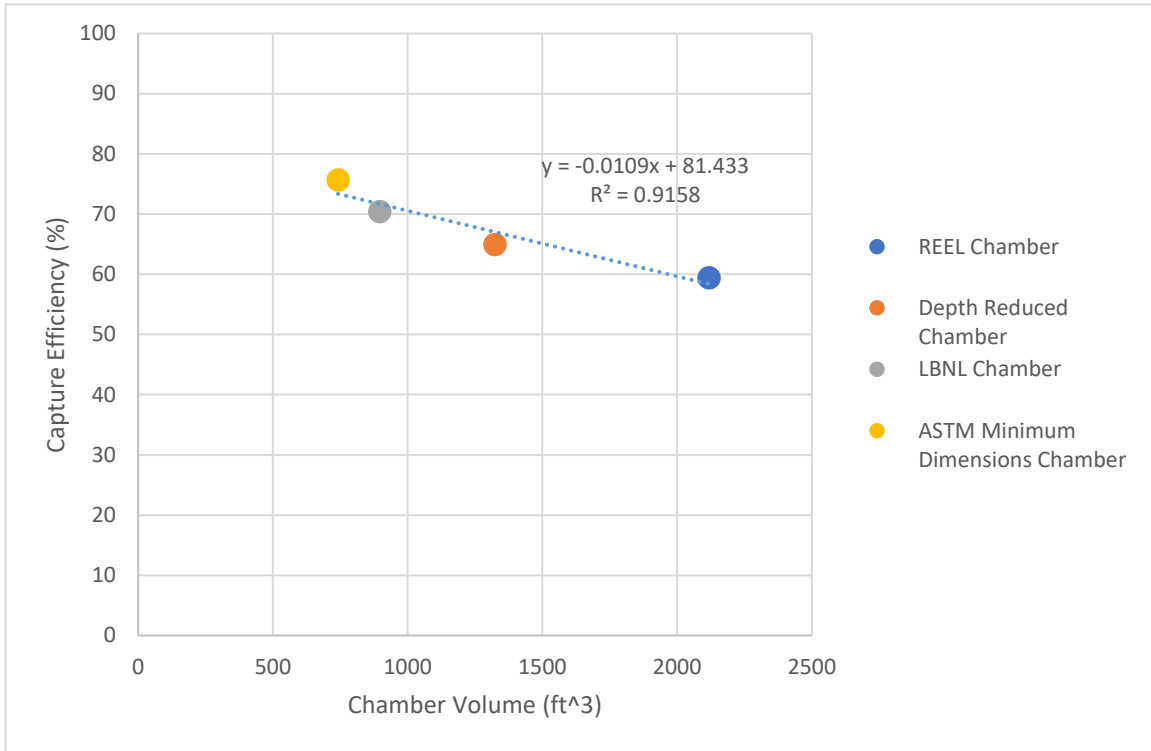


Figure 17: Calculated Range-hood CE Values varying with Volume Changes associated with the Four Simulations

It can be observed in Figure 17 that as the volume of the chamber decreases from the actual REEL test chamber to the minimum requirement volume specified in ASTM-E3087, then the capture efficiencies as predicted by the CFD simulation model increases to a maximum value, which was also observed in previous bar-charts and table. Also observed earlier and shown now in Figure 17 is that the REEL chamber as built and operated has the largest volume while also having the lowest CE value, compared to the other chambers. Another important observation in Figure 17 is that CE and volume have

an inversely proportional relationship with the curve plotted being almost linear, as evidenced by a linear curve fit having an  $R^2$  of 0.92.

The substantial difference in CE results obtained for different chamber volumes in this CFD simulation study confirms that the REEL and LBNL chambers, with their differing volumes, should not be expected to produce the same CE test results for the same fan unit even if test conditions are similar. It can also be concluded that if the CE test results from various test labs are to be consistent and comparable then it is imperative that the standard ASTM-E3087 should specify an exact chamber size, rather than simply specifying a minimum chamber size.



## CHAPTER 7. CONCLUSIONS

Domestic range-hoods were invented and designed for the purpose of maintaining healthy indoor air quality by removing steam and cooking contaminants, which can be emitted from food or from fuel combustions. The capture efficiency (CE) of a range-hood is defined as the ratio of pollutants that are captured or exhausted by a range-hood to those pollutants released in the kitchen environment. The standardized testing procedure for measuring the CE of range-hoods is outlined in ASTM-E3087. This thesis presents the development of a computational fluid dynamics (CFD) simulation model of turbulence mixing flow in the REEL test chamber, with the model and chamber both based on the CE test procedure specified in ASTM-E30878. The CFD model was designed to simulate the actual environment and conditions of the test chamber in order to study the mixing of the air inside the chamber. Other important and necessary parts of this research is to use the CFD simulation model, once it was validated, to determine the optimum location for measuring CO<sub>2</sub> concentrations during CE testing and, even more importantly, to study the effects of chamber volume on capture efficiency measurements, especially since the ASTM does not specify a chamber volume for testing.

First, the CFD model was validated by performing a series of simulations at three different operating speeds with each speed having a corresponding tracer gas (CO<sub>2</sub>) injection rate. The predicted values from the CFD simulation were compared with experimentally measured values taken using the actual CE test chamber at the lab. These comparisons showed that for all three fan speed cases, both the experimental method and the CFD simulation model produce similar capture efficiency (CE) results. The CFD

simulation results for the three cases differ from experimental measurements by only 0.01%, 2.73%, and 0.14%, demonstrating that the CFD model is capable of providing CE results that are consistent with measured values that utilize ASTM-E3087.

After validation, the CO<sub>2</sub> concentration distribution inside the chamber was analyzed, using the CFD simulation model, to find the sampling location inside the chamber that is the most optimum for a capture efficiency (CE) of range-hoods. The results of simulations showed that the CO<sub>2</sub> tracer-gas sampling location at the centerline of the test chamber and about 1.7 feet (0.5 m) away from the countertop table is optimum, in that the CO<sub>2</sub> concentrations here is representative of the chamber as a whole.

Finally, the CFD model was used to perform an investigation into the effect of the test chamber volume on capture efficiency measurements. A series of simulations were performed for four different sized CE testing chambers, namely the actual REEL test chamber, a chamber similar to the REEL chamber but with a depth reduction, an LBNL chamber, which is the only other chamber ever constructed and operated, and lastly, the standard minimum-dimension chamber specified in ASTM-E3087. These four simulations were run at the same operating speed of 160 CFM and at the same injection rate of 20 l/m. The result was a capture efficiency value of CE = 75.7% for the standard minimum-dimension chamber specified in ASTM-E3087, which is the highest value of the four chambers. For example, the CE for this minimum-dimension volume chamber is higher than the CE value calculated for the actual REEL chamber by about 27%. Based on the above results and discussions, a major contribution of this study is that if the CE test results from various test labs are to be consistent and comparable, then the standard

should specify an exact chamber size rather than simply specifying a minimum-dimension size chamber, which allows a chamber to be built with any volume as long as it is above the minimum.

## REFERENCES

- [1] ASTM E3087 - 18. ASTM INTERNATIONAL - STANDARDS WORLDWIDE. (2019).  
[HTTPS://WWW.ASTM.ORG/STANDARDS/E3087.HTM](https://www.astm.org/standards/E3087.htm).
- [2] ANSYS, INC. 2013. ANSYS® FLUENT, RELEASE 15.0, THEORY GUIDE, ANSYS, INC.
- [3] ANSYS, INC. 2013. ANSYS® FLUENT, RELEASE 15.0, USER'S GUIDE, ANSYS, INC.
- [4] CALIFORNIA AIR RESOURCES BOARD. INDOOR AIR POLLUTION FROM COOKING | CALIFORNIA AIR RESOURCES BOARD.  
[HTTPS://WW2.ARB.CA.GOV/RESOURCES/DOCUMENTS/INDOOR-AIR-POLLUTION-COOKING](https://ww2.arb.ca.gov/resources/documents/indoor-air-pollution-cooking).
- [5] NIELSEN, P.V. 2004. COMPUTATIONAL FLUID DYNAMICS AND ROOM AIR MOVEMENT.
- [6] INDOOR AIR 14 (SUPPLEMENT 7), 134–143.
- [7] NORTON, T. AND SUN, D.-W. 2006. COMPUTATIONAL FLUID DYNAMICS (CFD) – AN EFFECTIVE AND EFFICIENT DESIGN AND ANALYSIS TOOL FOR THE FOOD INDUSTRY: A REVIEW.
- [8] TRENDS IN FOOD SCIENCE & TECHNOLOGY 17, 600–620.
- [9] SHAH S., DUFVA K., (2017). CFD MODELING OF AIRFLOW IN A KITCHEN ENVIRONMENT : TOWARDS IMPROVING ENERGY EFFICIENCY IN BUILDINGS. , IN: XAMK TUTKII 1, KAAKKOIS-SUOMEN AMMATTIKORKEAKOULU. URN:ISBN:978-952-344-022-7
- [10] “RANGE HOODS: IU600ES - INSPIRA.” VENMAR, [WWW.VENMAR.CA/115-RANGE-HOOD-IU600ES-ISPIRA.HTML](http://WWW.VENMAR.CA/115-RANGE-HOOD-IU600ES-ISPIRA.HTML).